# *Chapter 6*

# *Determining endocrine disruptors from water by concentration and derivatization in PDMS multichannel traps*

## *6.1. Our approach*

The PDMS MCT consists of an open tubular assembly, making it suitable for the concentration of analytes directly from water, without the need for prior filtration. The PDMS MCT has already been utilized to concentrate PAHs from water [63, 67]. Since the analytes had no functional groups which could interfere with the chromatography, no additional sample preparation was required other than the removal of water from the trap before thermal desorption into the GC-MS [63, 67]. In order to extend the range of compounds amenable to PDMS MCT sampling, we decided to extract analytes that would require derivatization before analysis by GC-MS.

As described in chapter 1, there is a need to analyse ultra trace endocrine disruptors from water. Due to their extremely lipophyllic nature, estrogens and alkylphenols should, in theory, partition into PDMS MCT traps very easily. However, they possess hydroxyl functional groups, which require derivatization not only to improve the chromatography but also, perhaps simultaneously, to improve the detection properties of these analytes.

It is understood that, due to their lipophilicity, that the estrogens and alkylphenols are more likely to be adsorbed to particulates, sediments and sludge present in water sources. For example, literature indicates that approximately 50-75% of NP is adsorbed on sediment, implying only 25-50% is present in the water [9]. In addition estrogens may also occur as their glucuronide or sulphate conjugates resulting from human excretion [24, 58], the conjugates are not biologically active but are reconverted to free steroids by bacteria in the environment [276]. Thus the estrogens are largely deconjugated in water systems. The scope of this study did not include the investigation of the total content of these analytes in the water source, but to demonstrate the concentration of the free analytes in water in the PDMS MCT.

Ideally, for sampling, the PDMS MCT should be located where it can concentrate the analytes directly from the source, e.g. in a river. Following concentration the trap can be returned to the lab for further treatment without loss/change of the sample. Once in the lab, water can be removed from the trap and the derivatization reaction can be performed *in situ*, followed by thermal desorption and GC/MS analysis.

The first step in this study was to select a suitable derivatization reagent for the analytes and to determine how well the reaction would proceed within the PDMS matrix. Then the completeness of transfer of the derivatives from the trap (i.e. complete thermal desorption) to the column was verified. Once this was known, extraction efficiency of the analytes into the PDMS could be investigated. The steps were carried out in this order since it was impossible to analyse the extracted-underivatized analytes by comparison as their chromatographic performance deteriorates rapidly even when starting with a new GC column. Once concentration and derivatization have been demonstrated, the PDMS MCT could be applied to the analysis of real samples.

Table 6.1 lists the structures of the analytes to be determined in our study.

## *6.2. Derivatization*

### *6.2.1. Initial derivatization reactions involving the estrogens*

BSTFA leads the way as the derivatization reagent of choice for the conversion of hydroxyl groups on estrogens and alkylphenols [1-3, 21, 23-25, 243], (see chapter 3 page 63). However, it has been demonstrated that unless the ratio of BSTFA/ 1% TMCS/ pyridine, is not carefully regulated, the β-ethinylestradiol (EE2) derivative readily converts to the estrone (E1) derivative which is often being analysed simultaneously [244, 245].

It was therefore decided to rather perform an acylation reaction to convert the EDCs. This has the added advantage that anhydrous conditions are not required (see chapter 3). According to the results obtained by L. Dehennin *et al.* [246], shown in table 6.2, a maximum electron capture detector (ECD) response is obtained when the hydroxyl group on testosterone is substituted to form the heptafluorobutyrl (HFB) ester, followed closely by the pentafluorobenzoyl- (PFB) and pentafluorophenyl- (PFP) esters [246]. (See chapter 3 page 60, for derivatization reagents which yield these derivatives).

**Table 6.1 Endocrine disrupting compounds to be analysed by concentration and derivatization in the PDMS MCT.**

| Compound name: | Compound structure: | Molecular Formula: | Molecular Mass: | Abbreviation |
|---|---|---|---|---|
| 17β-estradiol | 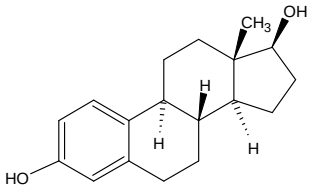 | $C_{18}H_{24}O_2$ | 272 | E2 |
| estrone | 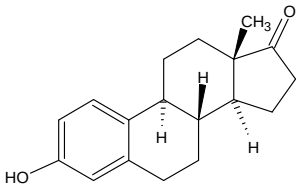 | $C_{18}H_{22}O_2$ | 270 | E1 |
| estriol | 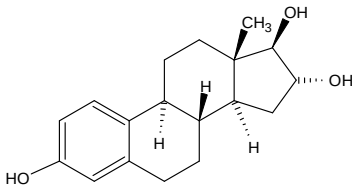 | $C_{18}H_{24}O_3$ | 288 | E3 |
| 17α-ethinylestradiol | 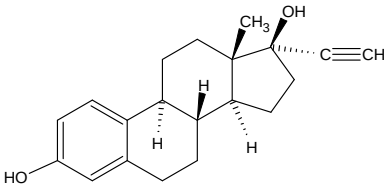 | $C_{20}H_{24}O_2$ | 296 | EE2 |
| 17β -testosterone | 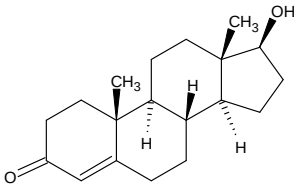 | $C_{19}H_{28}O_2$ | 288 | T |
| *tert*-octylphenol | 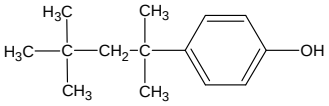 | $C_{14}H_{22}O$ | 206 | TOP |
| 4-n-nonylphenol | 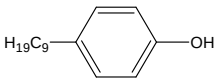 | $C_{15}H_{24}O$ | 220 | NP |
| bisphenol-A | 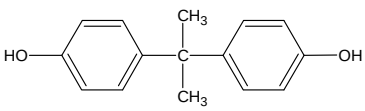 | $C_{15}H_{16}O_2$ | 228 | BPA |

From literature it was found that both the HFB and PFBCl reactions occur rapidly and would provide an electron rich derivative suitable for ECD and NCI-MS [62, 190, 192, 193, 247]. Both the HFB and PFBCl reactions required heating to 55ºC [62] and 80 ºC [191, 192, 247] respectively. However, certain methods have been described where no heating is required for either reaction [62, 193].

**Table 6.2 Comparison of electron-capture detector responses for different testosterone acyl-derivatives [246]. With permission from Preston Publications, IL, U.S.A.**

| Testosterone | R | Relative response |
|---|---|---|
| 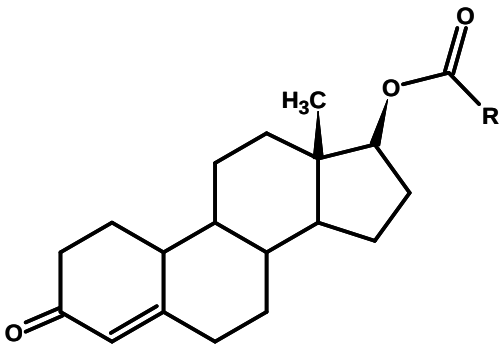 | $CH_3$ | 0.1 |
| | $CF_3$ | 0.4 |
| | $CH_2Cl$ | 4 |
| | $C_2F_5$ | 5 |
| | $C_3F_7$ | 19 |
| | $CF_2Cl$ | 34 |
| |  | 50 |
| | $C_7F_{15}$ | 60 |

[L. Dehennin, A. Reiffstock, R. Scholler; *J. Chromatogr. Sci*. (1972) 10, p 224]

## *6.2.2. Derivatization of the estrogens with Pentafluorobenzoyl chloride (PFBCl)*

Initial tests using PFBCl were attempted. Here the concept was to first derivatize the analytes in the water, then to hydrolyse the excess reagent to the acid (which would remain ionized in the aqueous phase) and extract only the derivatives into the PDMS MCT by pouring the entire sample reaction mixture through the trap. Both Akre, Fedeniuk and MacNeil [191] and Xiao and McCally [192, 247], derivatized the estrogens from water under anhydrous conditions i.e. the sample was first evaporated to dryness. The reaction with PFBCl occurred in organic solvents at elevated temperatures. A more elegant method was presented by Kuch and Ballschmiter [193], where the

reaction between PFBCl and the estrogens occur in water. The derivatives that form immediately, at room temperature, are extracted into hexane [193]. Excess PFBCl remains in the aqueous phase [193]. The latter reaction seemed appropriate for our PDMS MCT experiment. Identical steps could be followed until the final extraction step where the hexane (non-polar solvent) would be replaced by the PDMS MCT ("non-polar" solvent).

Attempts to synthesise the derivatives using the method by Kuch and Ballschmiter [193] were not successful. Only the hydrolyzed reagent was observed, implying that neither the estrogen nor the derivative was extracted into the hexane. It is possible that the reagent was old and already hydrolysed before being opened, thus a new reagent vial was opened but the process still yielded the PFB hydroxide. Figure 6.1 shows a typical chromatogram with mass spectrum of the main reaction product, obtained on a Micromass® GC-TOFMS. The product was confirmed using the NIST library mass spectrum.

Using the methods by Akre *et al* and Xiao *et al*, returned the same result. One of two explanations are possible, the most obvious being: i) the PFBCl reagents have all hydrolysed before the vial is opened; or ii) the reaction conditions, particularly in water or in solvents containing water have caused the PFBCl to hydrolyse, thus preventing the reaction from occurring. Further work with this reagent was abandoned, as time was limited at this stage.

### *6.2.3.Derivatization of the estrogens with trifluoroacetic acid anhydride (TFAA)*

Trifluoroacetic acid anhydride (TFAA) was used to convert both the phenolic and hydroxyl functional groups on the estrogens. The reaction was tested in the PDMS MCT as follows:
50 µl of a 20 ng/µl EDC mixed standard consisting of E1, E2, E3, EE2 and T (defined in table 6.1) in acetone, was inserted into the PDMS trap using a Drummond ® Microcap capillary (with plunger). The acetone was removed by gently blowing nitrogen gas through a capillary into the trap until acetone could no longer be detected by smelling the trap outlet (usually less than a minute of purging). 10 µl of TFAA was added to the bottom of the PDMS trap. The PDMS MCT was then sealed at both ends with glass plugs and the reaction allowed to proceed for 10 minutes. The trap was then immediately thermally desorbed in the Chrompack ® TDU and analysed by GC-(EI) MS.

The instrument conditions were as follows:

Splitless desorption at 280ºC for 20 min with a desorb flow of 100 ml/ min, inject at 280ºC for 5 minutes. The GC oven was held at 40ºC for 1 min then ramped at 5º/min to 280ºC and held for 10 min, then ramped again at 20º/min to 300ºC and held for 5 min. A solvent delay of 28 min was set on the MS to avoid the detector being damaged by the excess volatile TFAA entering the MS. A scan range of 40 – 600 amu was used.

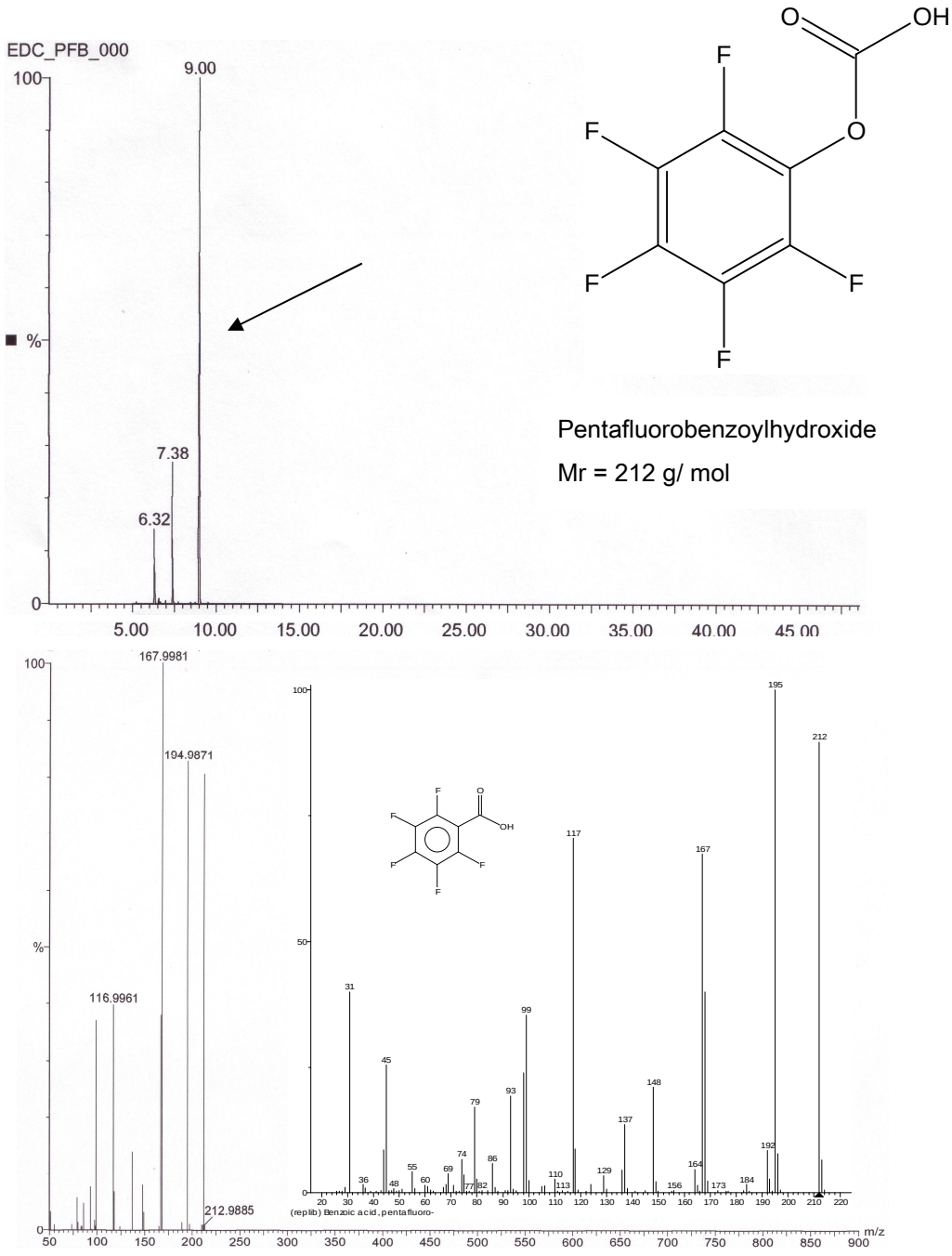


**Figure 6.1. Gas chromatogram and time-of-flight mass spectrum of PFBCl hydrolysis product obtained when performing the method introduced by Kuch and Ballschmiter [193].**

Figure 6.2 shows the total ion chromatogram (TIC) obtained for this experiment. The TIC for the desorbed PDMS MCT trap shows extremely overloaded and jagged-edged PDMS thermal degradation peaks reflecting the excess TFAA reagent and very high thermal desorption temperature used. It should be noted that the chromatogram using NCI-MS (shown in figure 6.8 below) is significantly cleaner since the PDMS degradation peaks are selectively removed because of poor ionization with the NCI technique.

The reconstructed ion chromatogram (RIC) of the molecular ions of each derivative observed is shown beneath the TIC in figure 6.2. The RIC gives a good indication of how the selectivity of the MS improves when moving to Selected Ion Monitoring (SIM) – where the PDMS thermal degradation peaks are absent.

Figures 6.3 to 6.6 show the EI mass spectra obtained for the E2, E1, E3 and T – TFA derivatives each with an abundant molecular ion. Both hydroxyl and phenol groups were substituted to form the TFA ester. The presence of the TFA moiety in each derivative is confirmed by m/z 69 ($-CF_3$). Out of interest, another peak not shown on the RIC is the enol tautomer of testosterone that is doubly substituted with TFA. Figure 6.7 shows the mass spectrum of the disubstituted derivative together with the keto-enol tautomerism occurring with testosterone. The disubstituted E2 TFA derivative and the T derivative mass spectra agree with the corresponding mass spectra provided by Lerch and Zinn [62]. *Mass spectra for most of the estrogen-TFA derivatives were not available in the NIST or Wiley libraries*. Neither the mono-($M^+$ m/z 392) nor the di-TFA($M^+$ m/z 488) derivative of EE2 was observed, figure 6.2. The EE2-di-TFA derivative was expected to elute between the E1-TFA and T-TFA derivatives [62].

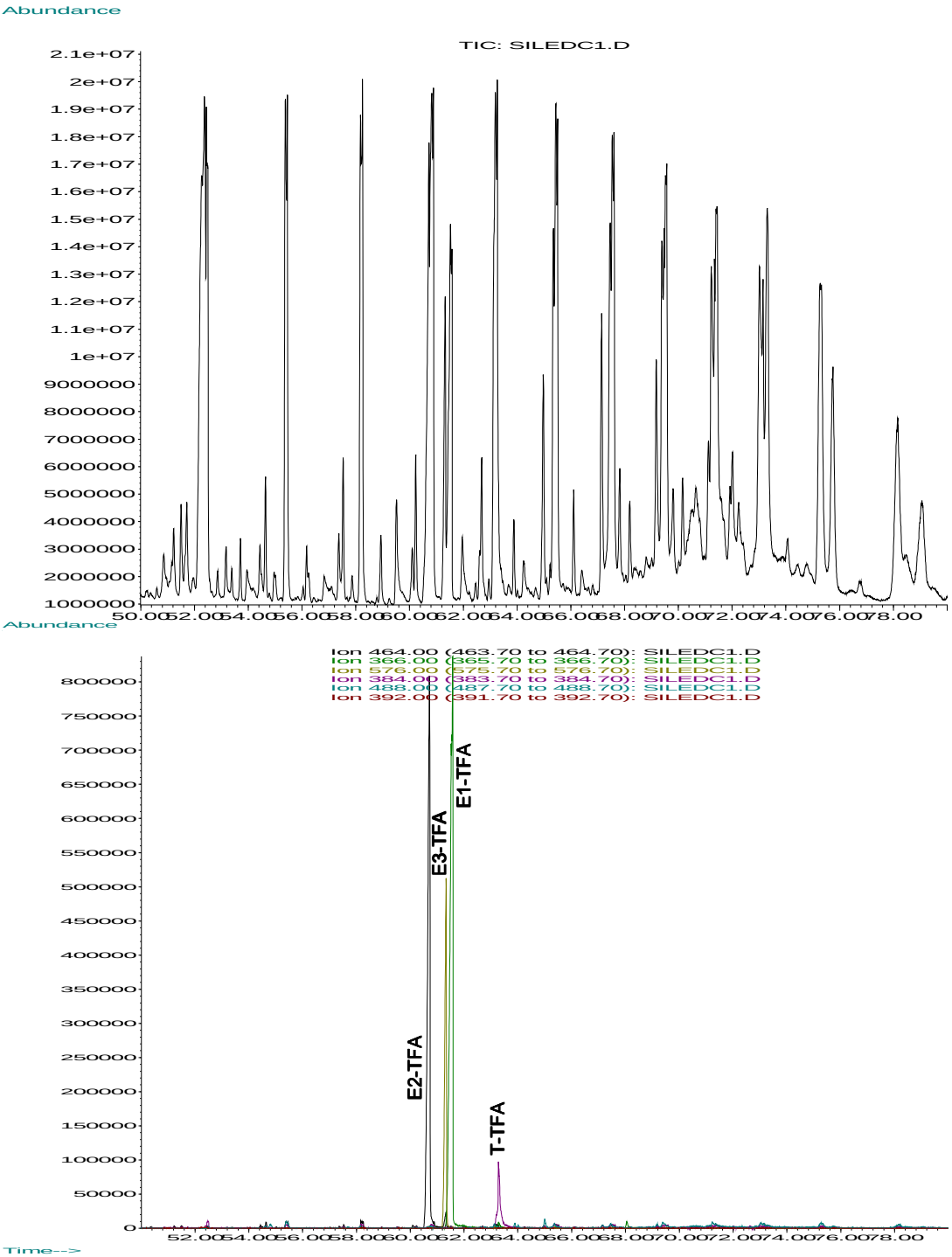


**Figure 6.2 GC- (EI) MS: Total ion chromatogram (TIC) of the *in situ* derivatization of estrogens in the PDMS MCT using TFAA. Beneath is the reconstructed ion chromatogram of molecular ions of the derivatives of : estrone (E1-TFA); β-estradiol (E2-di-TFA); estriol (E3-tri-TFA) and testosterone (T-TFA) trifluoroacetate (TFA) derivatives.**

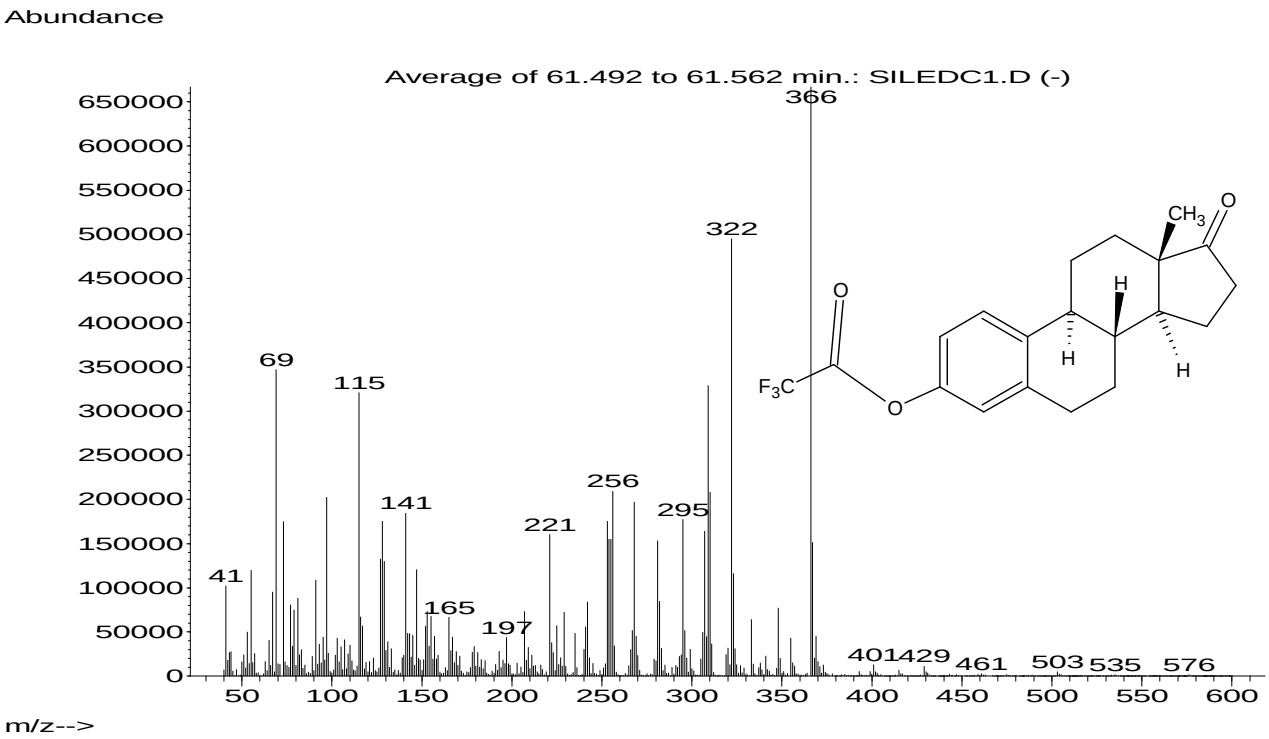


**Figure 6.3 Electron impact mass spectrum of the estrone-trifluoroacetate (E1-TFA) derivative. Molecular ion ($M^+$) m/z 366, ($-CF_3$) m/z 69.**

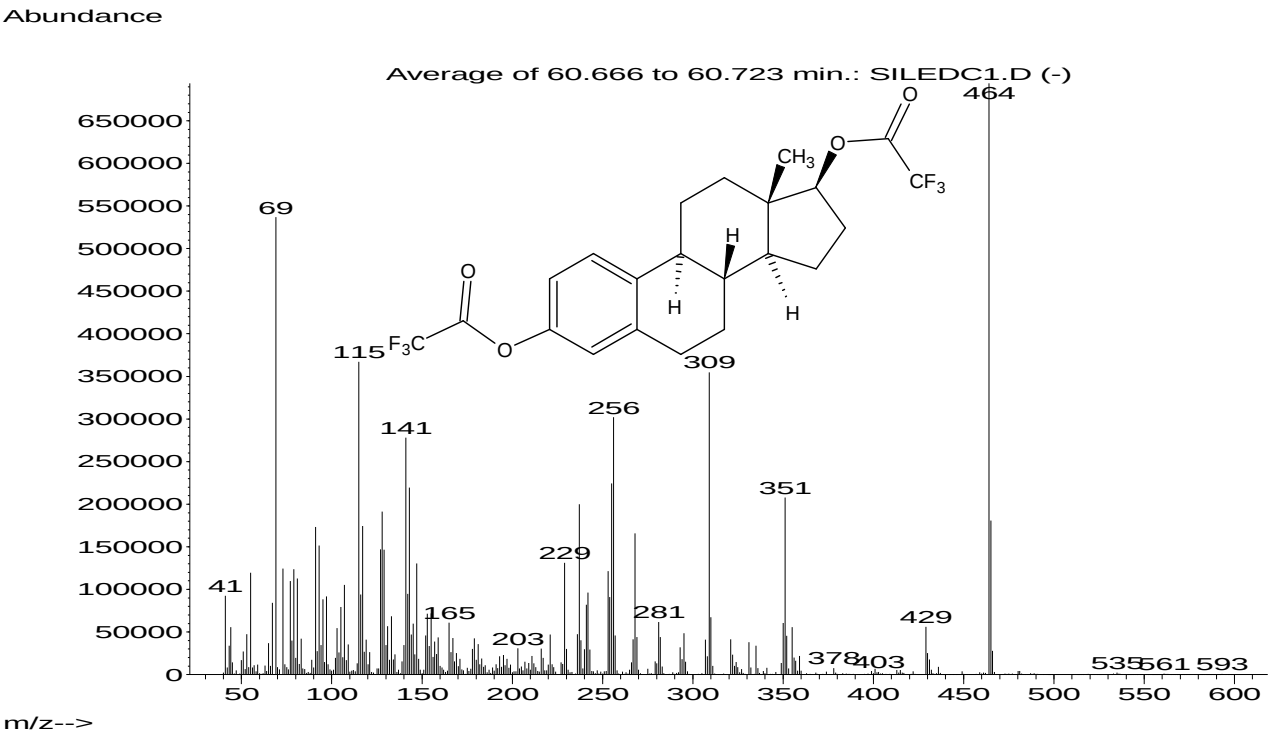


**Figure 6.4 Electron impact mass spectrum of the 17β-estradiol-trifluoroacetate (E2-di-TFA) derivative. Molecular ion ($M^+$) m/z 464, ($-CF_3$) m/z 69.**

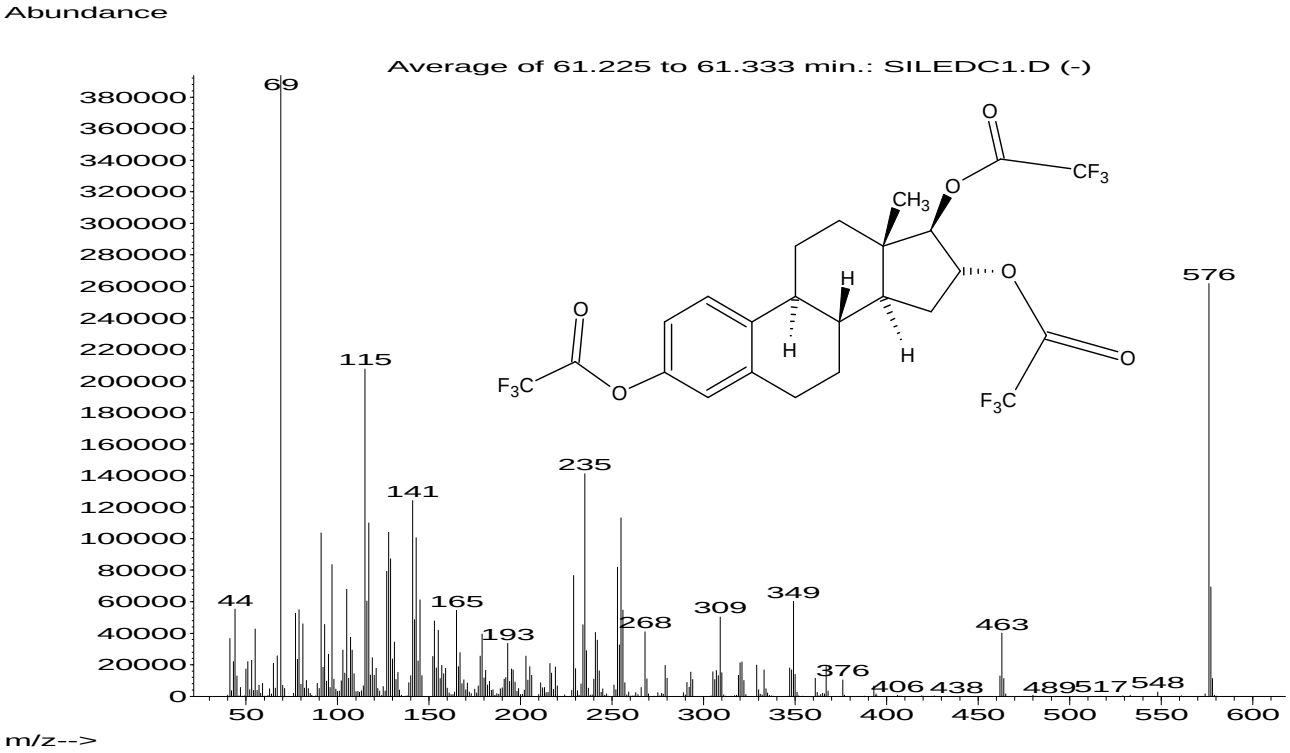


**Figure 6.5 Electron impact mass spectrum of the estriol-trifluoroacetate (E3-tri-TFA) derivative. Molecular ion ($M^+$) m/z 576, ($-CF_3$) m/z 69.**

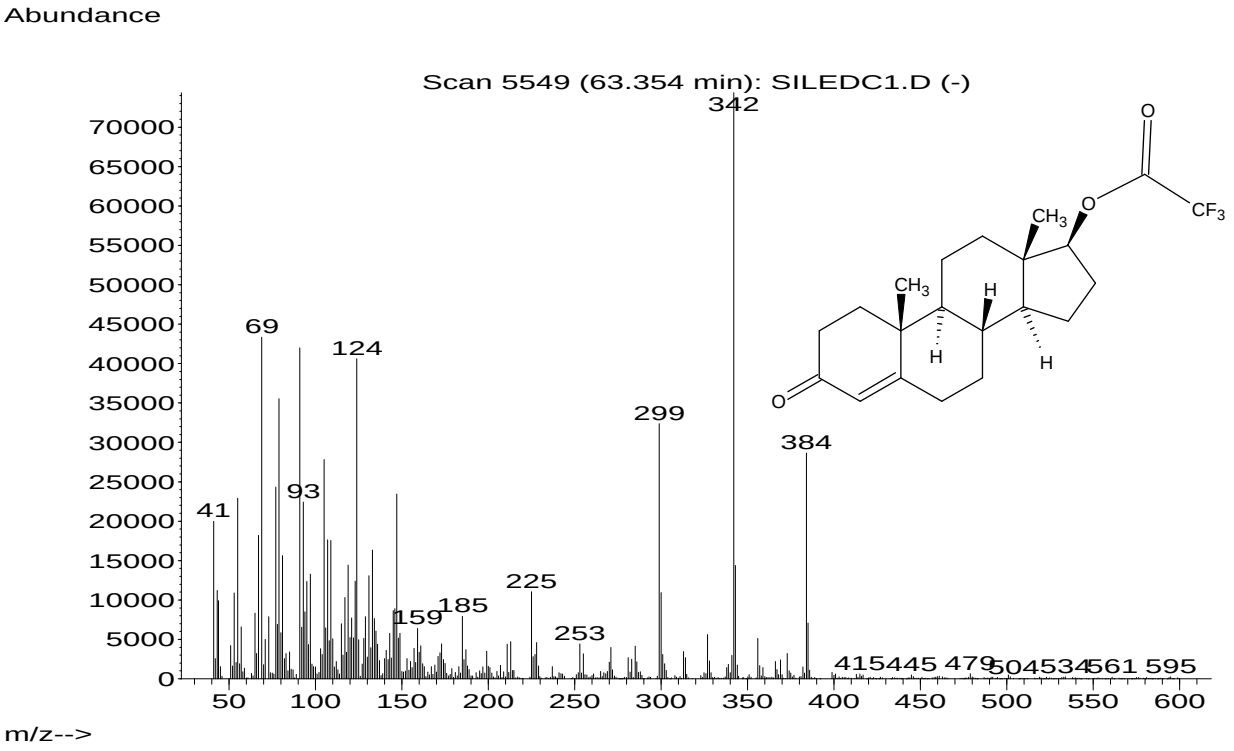


**Figure 6.6 Electron impact mass spectrum of the testosterone-trifluoroacetate (T-TFA) derivative. Molecular ion ($M^+$) m/z 384, ($-CF_3$) m/z 69.**

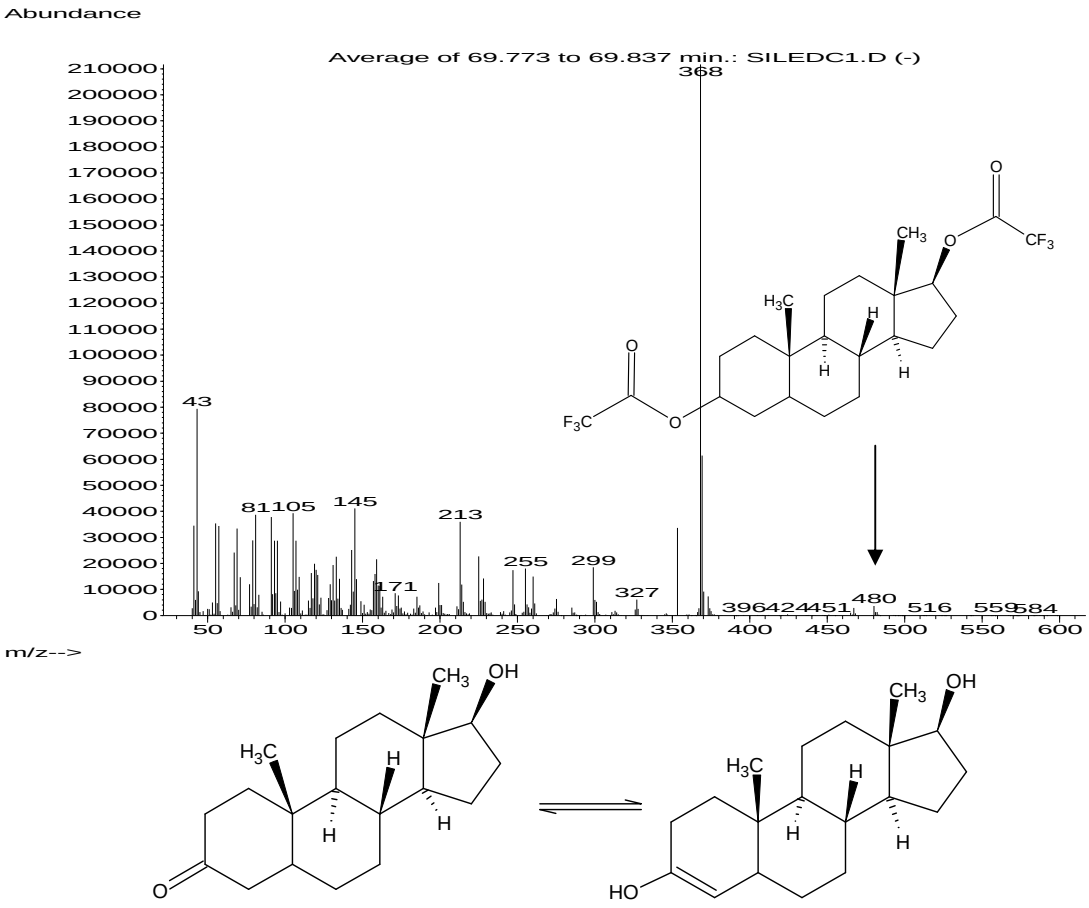


**Figure 6.7 Electron impact mass spectrum of the testosterone-ditrifluoroacetate (T-di-TFA) derivative. Molecular ion ($M^+$) m/z 480, ($-CF_3$) m/z 69. Beneath the mass spectrum is a sketch of the equilibrium between the ketone and enol tautomers of testosterone.**

The estrogen TFA derivatives were again synthesised on the trap as described earlier. The trap was then immediately thermally desorbed in the Chrompack ® TDU and analysed by GC-(NCI) MS. Figure 6.8 shows the TIC obtained by GC (NCI) MS. Beneath the TIC is the RIC of m/z 113, which corresponds to the mass of the trifluoroacetate ion $-CF_3CO_2^-$. It appears that several more TFA derivatives are detected by NCI-MS. Most of these chromatographic peaks only have a base mass peak of m/z 113 with no other ion information available to identify them. Peaks having other ions in addition to m/z 113 are m/z 488 and m/z 576 as shown in the subsequent RICs and figure 6.9 below.

Figure 6.9 shows the NCI-Mass Spectra for one of many peaks in the chromatogram with base peak m/z 113, followed by the NCI-mass spectrum for the suspected EE2-TFA derivative and E3-TFA derivative. At the elution time for E3-TFA (~61 min), the molecular ion m/z 576 appears. This is unusual for NCI using methane gas, where (M-1) is expected. It is suspected that EE2-TFA (not present in EI-MS) with a base peak of m/z 488 and fragment ion m/z 113 is observed much earlier

in the chromatogram (~37 min). This suggests that the supposedly sterically hindered α - hydroxyl group can be substituted. Several publications and reviews in literature have stated that this hydroxyl group is not substituted by most acylation reagents, due to the hindrance of the alkyne substituent adjacent to the hydroxyl functional group [199]. BSTFA has formed the TMS ester on both aromatic and alkyl substituent, although this was not confirmed by all research groups [199]. The TMS derivatives are also more susceptible to hydrolysis [3, 199]. Notice that m/z 113 is the base peak, when using methane as collision gas [62]. If using water as collision gas, then the molecular ion is expected to be the base peak [62]. This would be a better setup with NCI, since m/z 113 lies very low on the mass scale thus not improving the selectivity of detection. Moving into higher mass ranges would improve the selectivity of the detection technique.

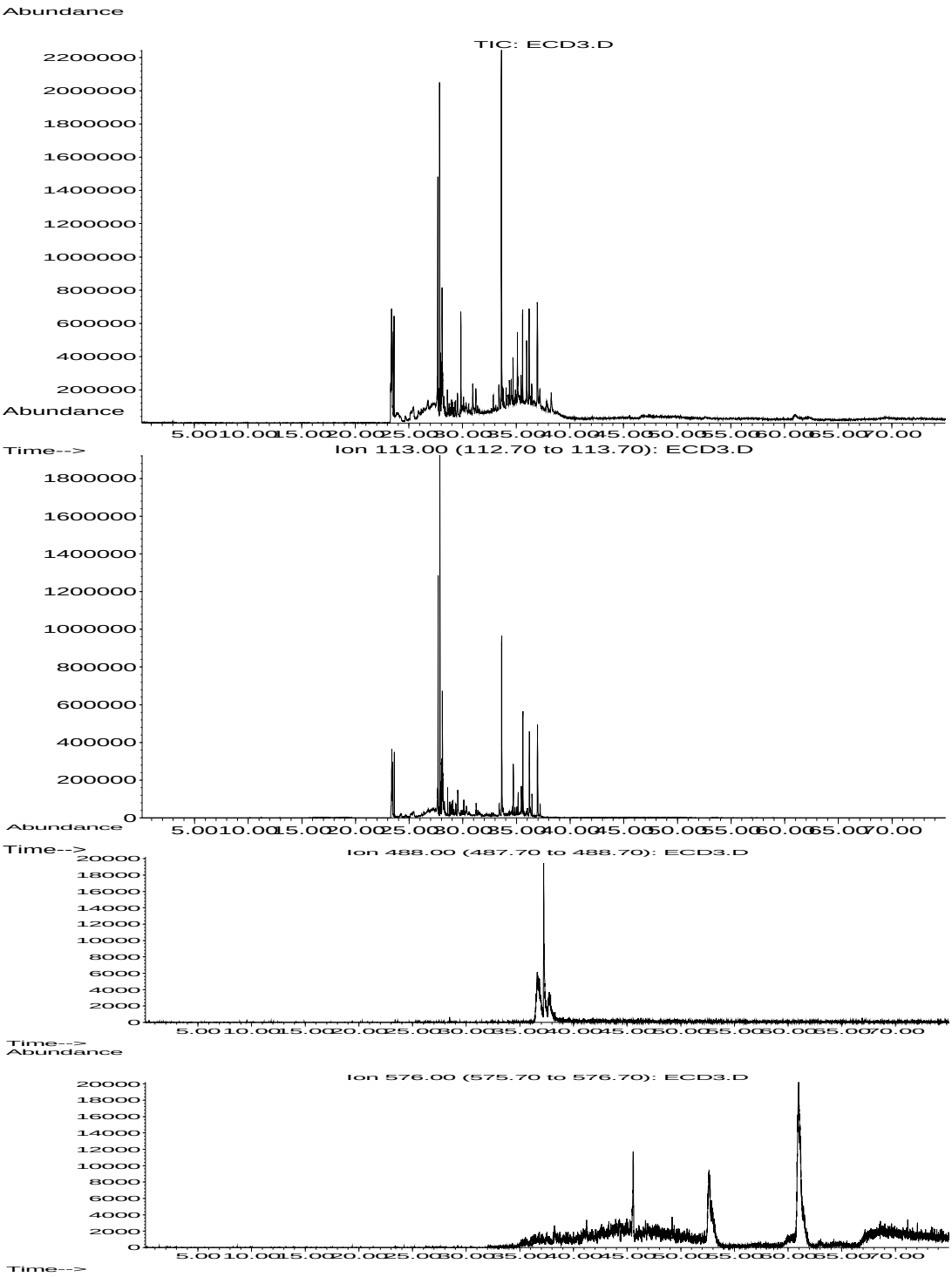


**Figure 6.8 The TIC obtained from GC- (NCI) MS of the *in situ* derivatization of estrogens in the PDMS MCT using TFAA, followed by the RIC for m/z 113, indicating all peaks having the trifluoroacetate ion, m/z 488 RIC, indicating the suspected EE2-di-TFA derivative peak eluting at 37 min and m/z 576 RIC indicating the suspected E3-tri-TFA derivative peak eluting at 61 min .**

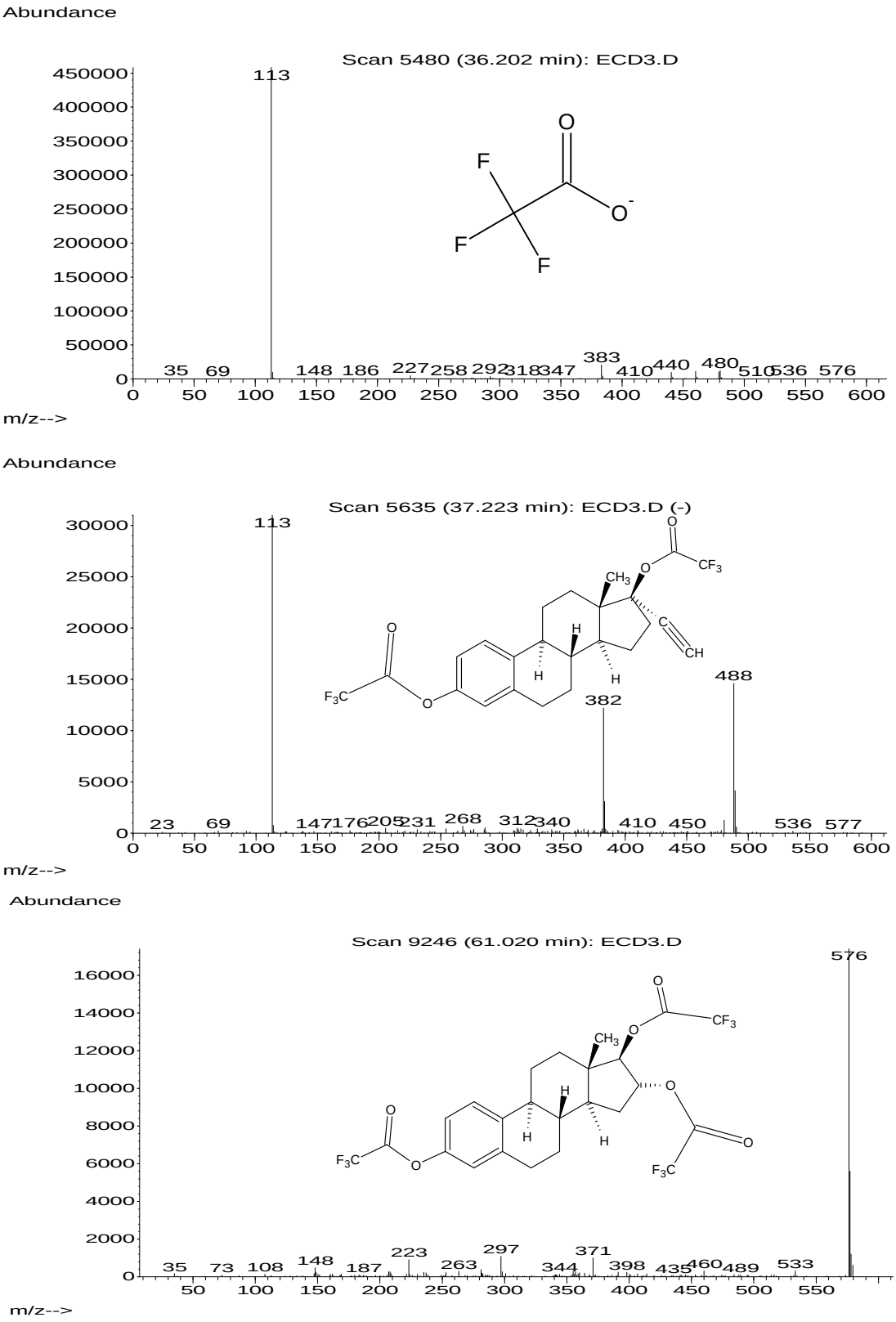


**Figure 6.9 The negative chemical ionization-mass spectra (NCI-MS) for one of many peaks in the chromatogram with base peak m/z 113, followed by the NCI-mass spectrum for the suspected EE2-di-TFA derivative ($M^-$ m/z 488) and E3-tri-TFA derivative ($M^-$ m/z 576).**

Further investigation of the EE2-di-TFA derivative was performed on the GC-ITD (the instrument available at the time of the study). Here 1 µl of an 8 µg/µl EE2 standard in acetone was placed in an empty glass tube. 1 µl of TFAA was added; the glass tube was sealed with glass caps and allowed to react for 10 min. The tube was then immediately thermally desorbed in the Chrompack ® TDU and analysed by GC- (ITD) MS. The instrument conditions were as follows:

Splitless desorption at 280ºC for 10 min with a desorb flow of 100 ml/ min, inject at 280ºC for 1 minute. The GC oven was held at 40ºC for 1 min then ramped at 15º/min to 280ºC and held for 10 min. A solvent delay of 16 min was set on the MS to avoid the detector being damaged by the excess volatile TFAA entering the MS. A scan range of 40 – 600 amu was used.

The chromatogram obtained showed the presence of 5 major compounds present for the reaction of TFAA with EE2, figure 6.10. The reaction between TFAA and EE2 occurs in the absence of a basic catalyst resulting in extremely acidic reaction conditions. Under these conditions Wagner-Meerwein rearrangements [248, 249], figure 6.11, and dehydration reactions can occur. Figures 6.12 to 6.16 show the different derivatives of EE2-TFA formed under acidic conditions (in the presence of excess TFAA).

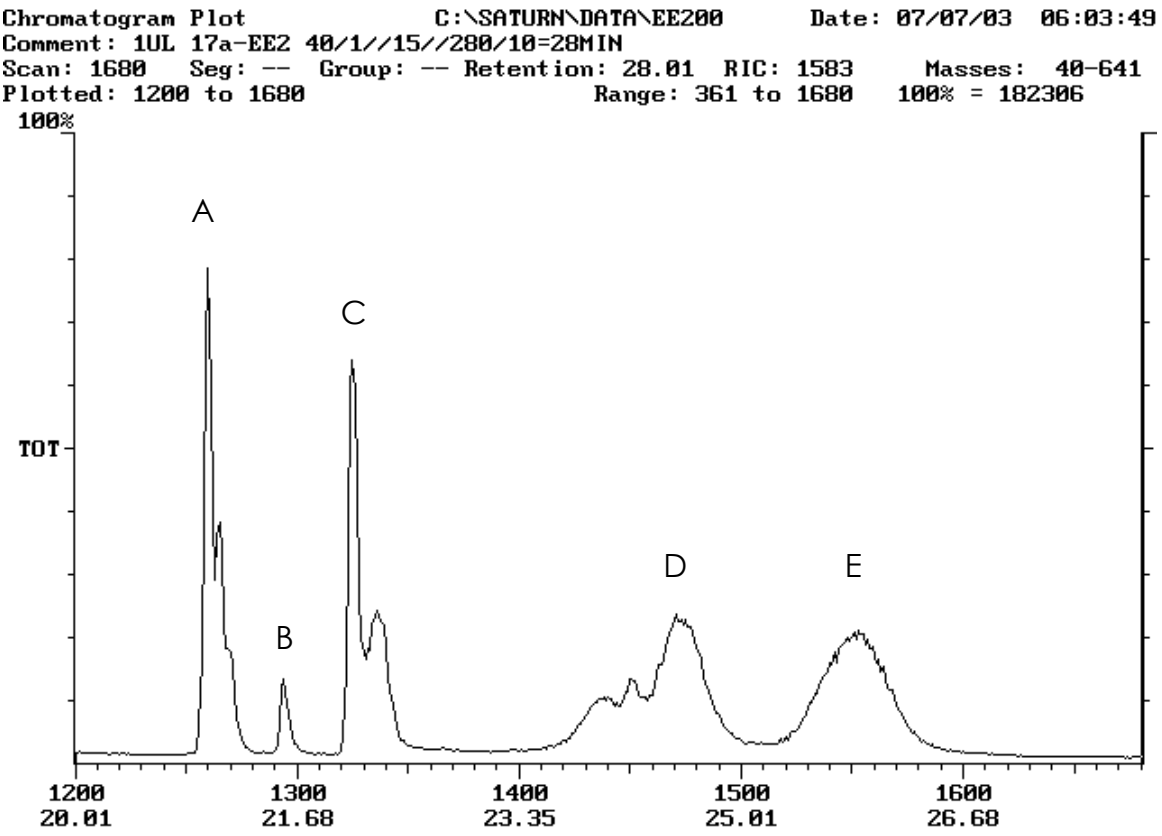


**Figure 6.10 The GC- (ITD) MS chromatogram obtained for the reaction of EE2 with TFAA in a glass tube. 5 major compounds, labelled A, B, C, D and E were identified for the derivative.**

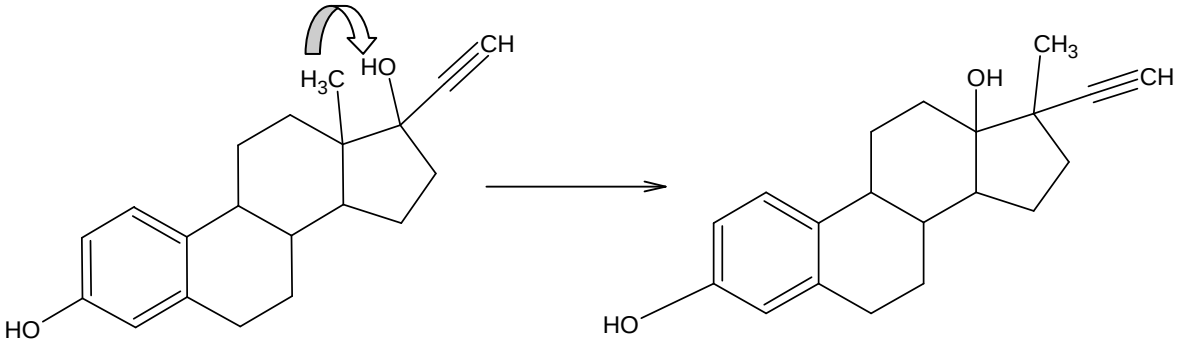


**Figure 6.11. 17α-ethinylestradiol (EE2) undergoing a Wagner Meerwein rearrangement, essentially this is a 1,2- shift between 2 groups on adjacent $sp^3$ hybridized carbon atoms [248, 249].**

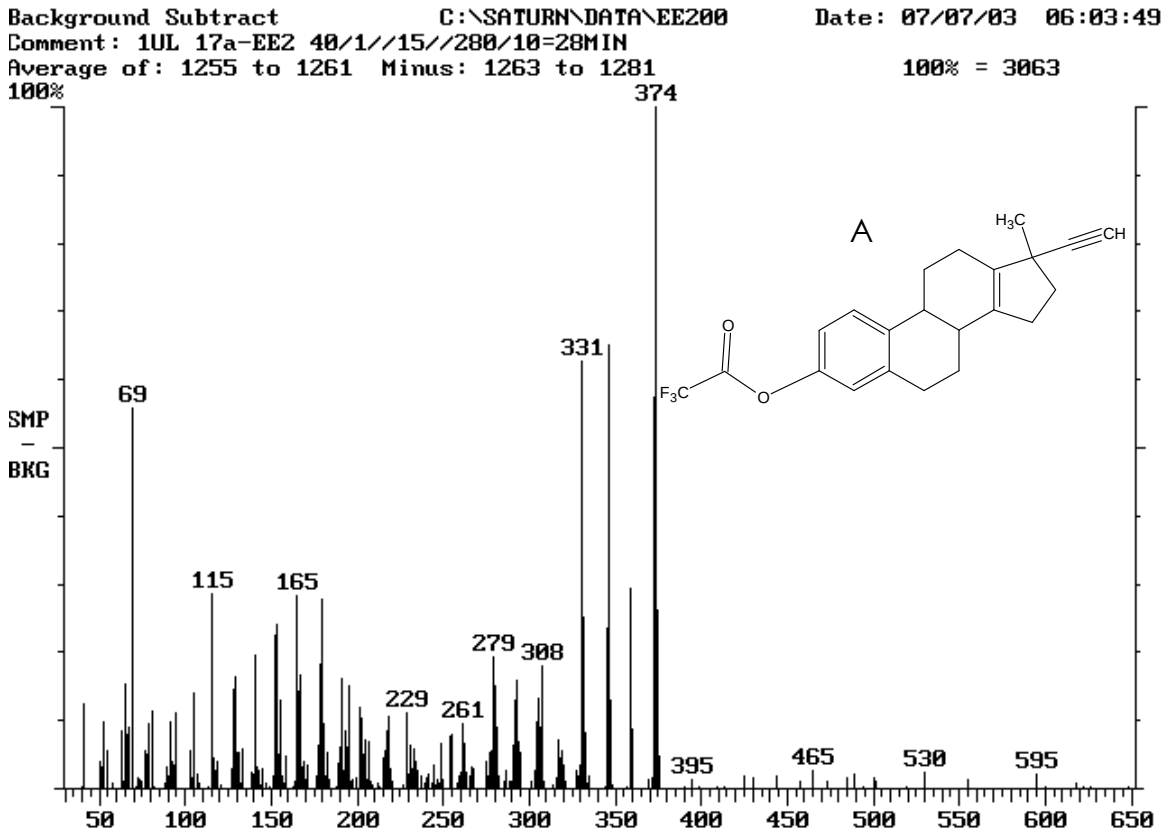


**Figure 6.12. The ITD-EI mass spectrum of compound A. The mono-substituted EE2-TFA derivative has undergone a Wagner-Meerwein rearrangement and a water elimination step (dehydration) to form a double bond between the C5 and C6 rings. The base peak m/z 374 is also the molecular ion $M^+$.**

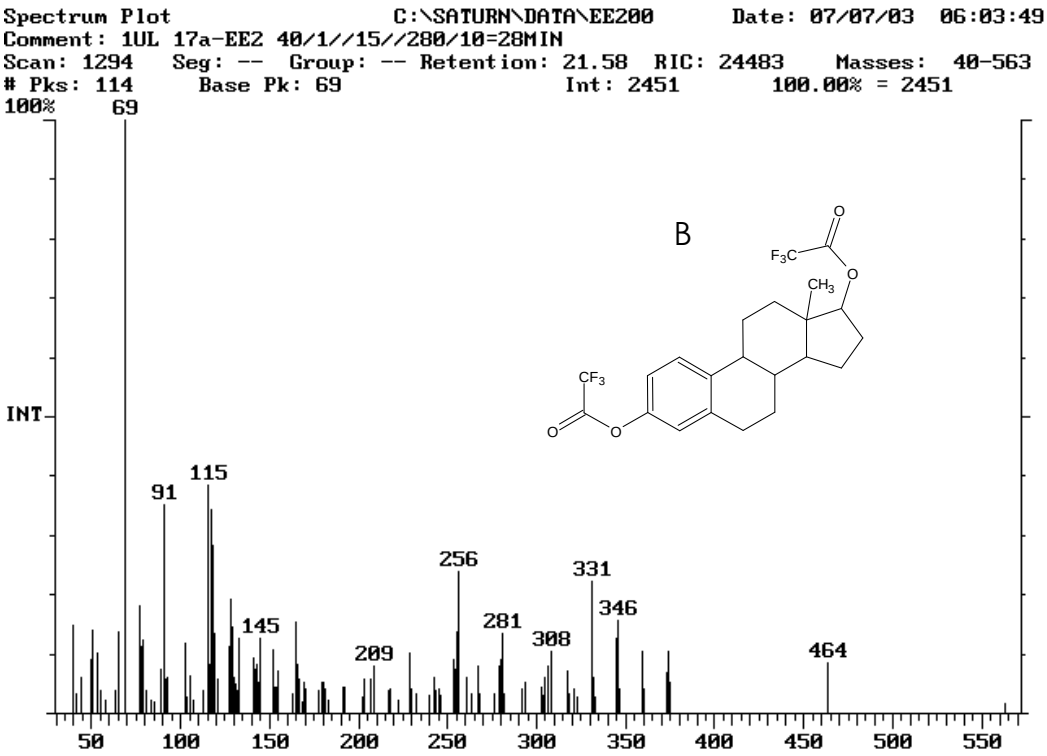


**Figure 6.13. The ITD-EI mass spectrum of compound B. The disubstituted EE2-TFA derivative has lost the 17-alkynyl (C-C) group (-24 amu).**

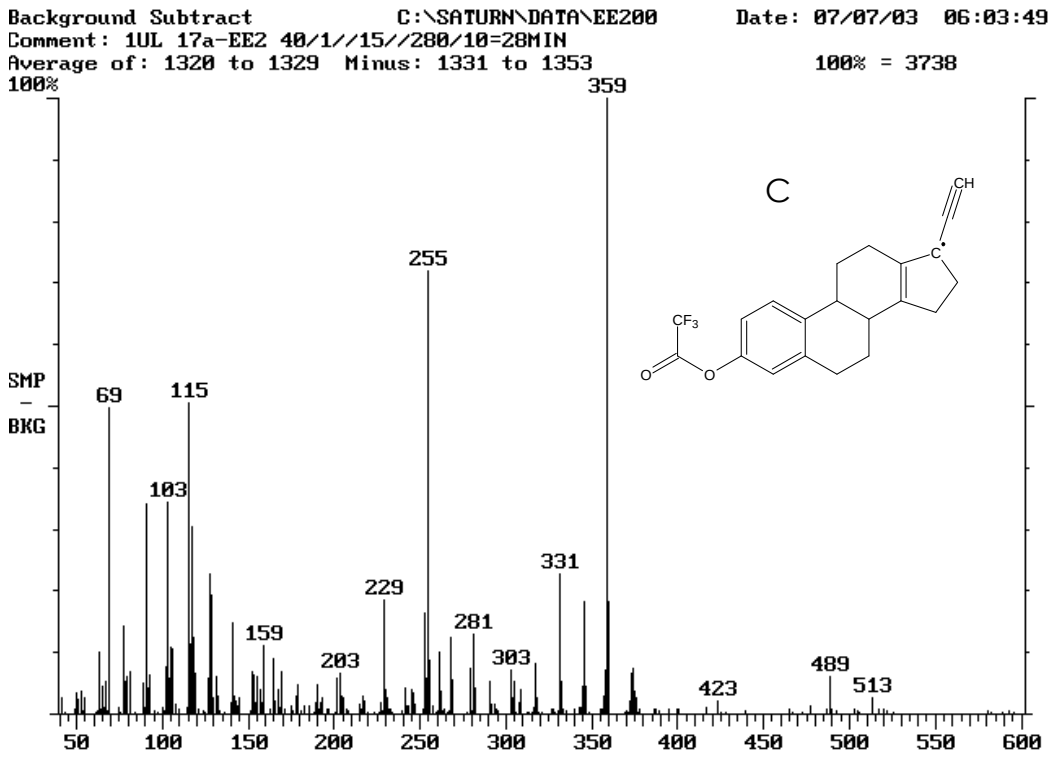


**Figure 6.14. The ITD-EI mass spectrum of compound C. The mono-substituted EE2-TFA derivative has undergone a Wagner-Meerwein rearrangement and a water elimination step (dehydration) to form a double bond between the C5 and C6 rings. The methyl group is lost to form base peak m/z 359 and molecular ion at m/z 374.**

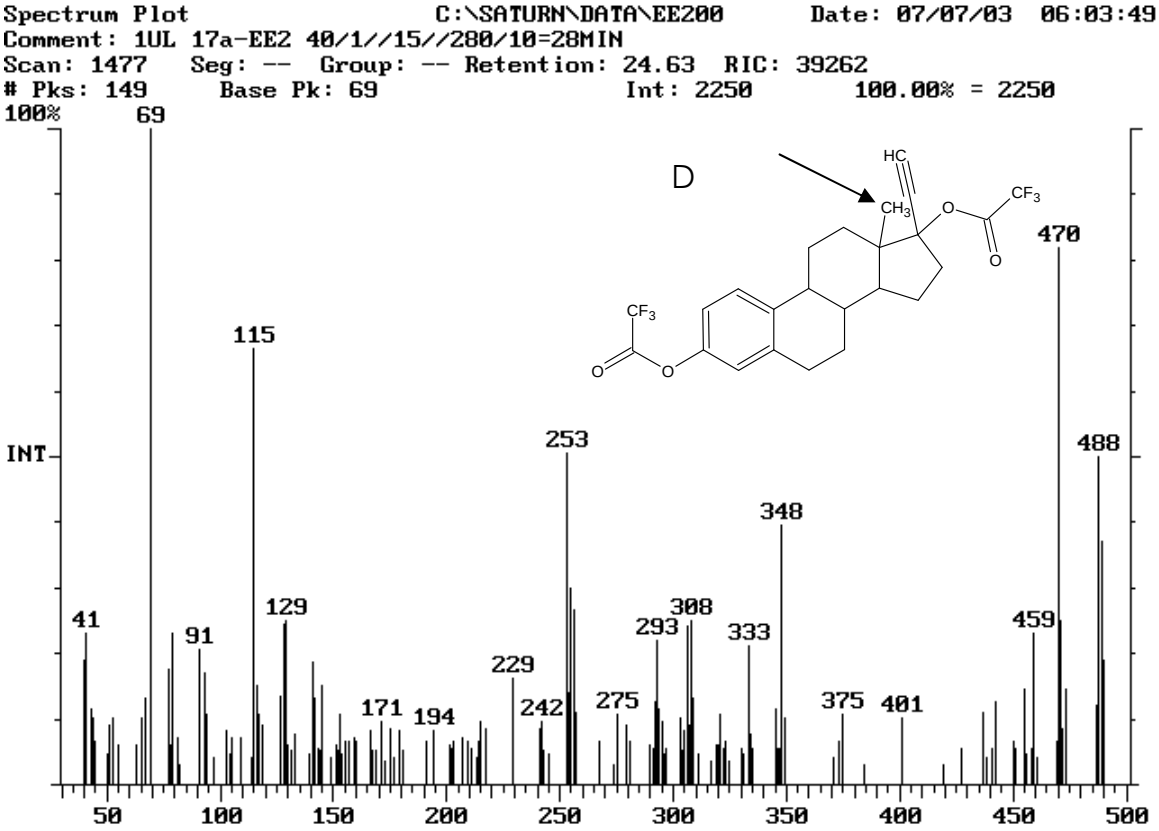


**Figure 6.15. The ITD-EI mass spectrum of compound D. The disubstituted EE2-di-TFA derivative.**

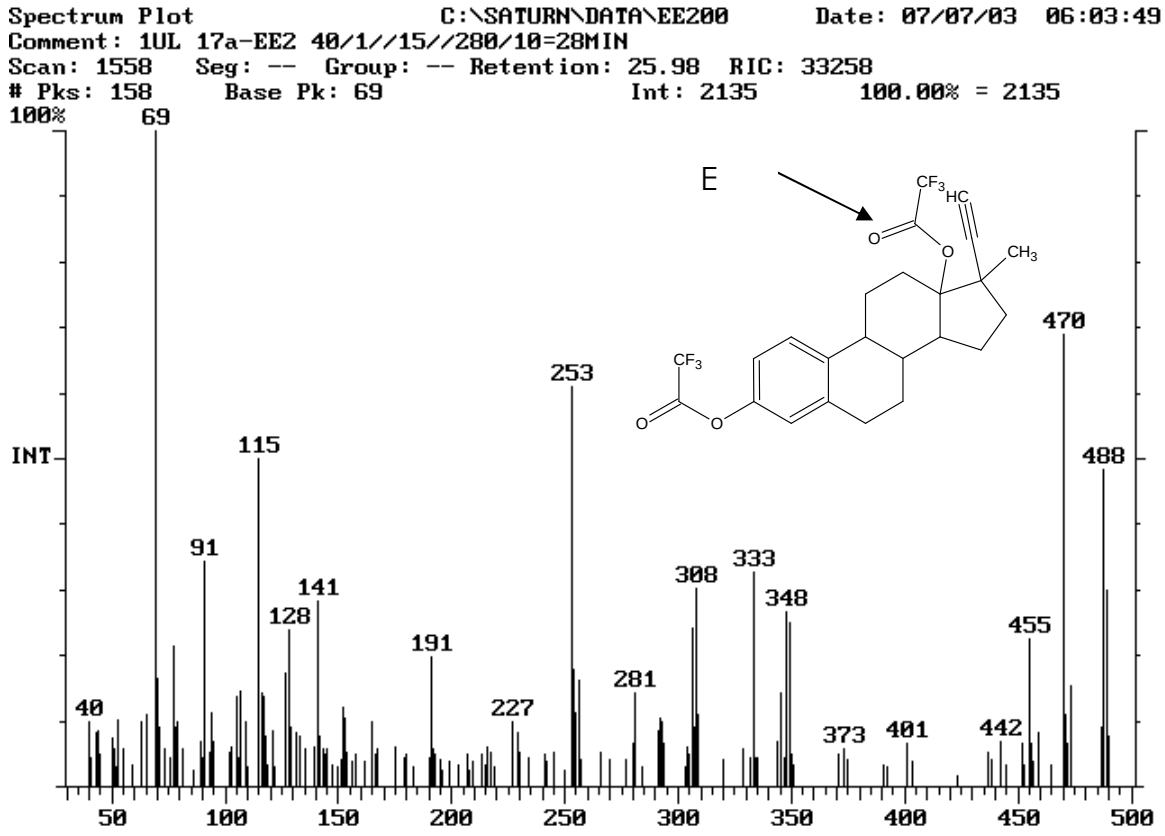


**Figure 6.16. The ITD-EI mass spectrum of compound E. The disubstituted EE2-di-TFA derivative after a Wagner Meerwein rearrangement.**

## *6.2.4. Dual derivatization of the estrogens with PFBCl and TFAA*

In view of the poor results obtained with the PFBCl and TFAA applied separately, as a last resort we decided to combine the reagents. In literature, dual derivatizations are performed to convert functional groups of different reactivity resulting from steric hindrance, as is the case for the hydroxyl group on EE2, which is hindered by the 17-alkynyl group [181].

A simple reaction in a vial with the 20 ng/ µl EDC standard in acetone, 5 µl TFAA and 5 µl PFBCl was performed. 1 µl of this reaction mixture was injected with a split into the GC- (EI) MS on full scan, with a solvent delay. Figure 6.17 shows the RIC of m/z 195 corresponding to the pentafluorophenyl carbonyl moiety. Although not shown here, the TIC looks similar to the RIC. Figures 6.18 to 6.20 show the 3 derivatives that formed successfully from the dual derivatization; unfortunately 17α-ethinylestradiol (EE2) was not among them. They are estrone (E1), estriol (E2) and estradiol (E3). It is important to note that the hydrolysed PFBCl (PFBOH) is also present (figure 6.21), as are the derivatives. The presence of both m/z 195 and m/z 69 in the mass spectra of the derivatives indicate that both the PFB and TFA moieties are present. The PFBCl reagent does in fact react with the estrogens. It would appear that it is not entirely hydrolysed in the reagent vial. Further investigation into the methodology required for synthesizing the PFB estrogen derivatives is needed. It remains the model route to follow for the detection of estrogens.

Due to time constraints and the fact that suitable derivatives of the estrogens (with either TFAA or PFBCl) were not achieved, this work was discontinued. The estrogen-TFA derivatives did not yield EE2-TFA on the PDMS MCT either at room temperature or during thermal desorption. The EE2-TFA derivative formed in the glass tube resulted in four products instead of one. The method used for the reaction of PFBCl with the estrogens was not successful. Further work was carried out using the alkylphenols only.

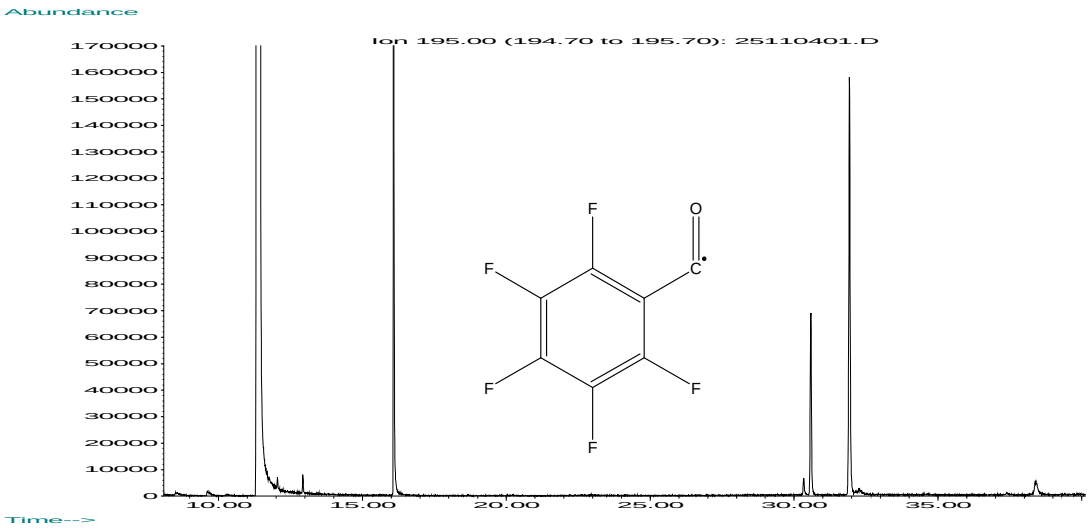


**Figure 6.17 The GC- (EI) MS Reconstructed ion chromatogram (RIC) of m/z 195 corresponding to the pentafluorophenyl carbonyl moiety, for the dual derivatization of estrogens with PFBCl and TFAA.**

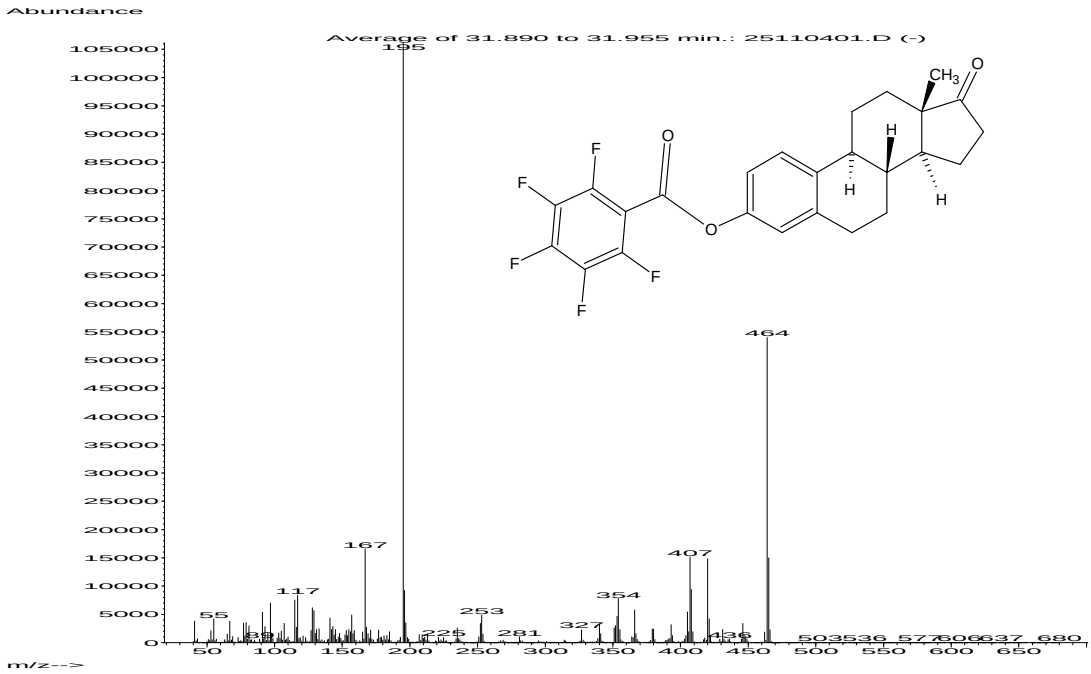


**Figure 6.18 The EI mass spectrum obtained for the derivative formed from the reaction of estrone (E1) with PFBCl and TFAA. Base peak m/z 195 ($C_7F_5O$) and $M^+$ m/z 464.**

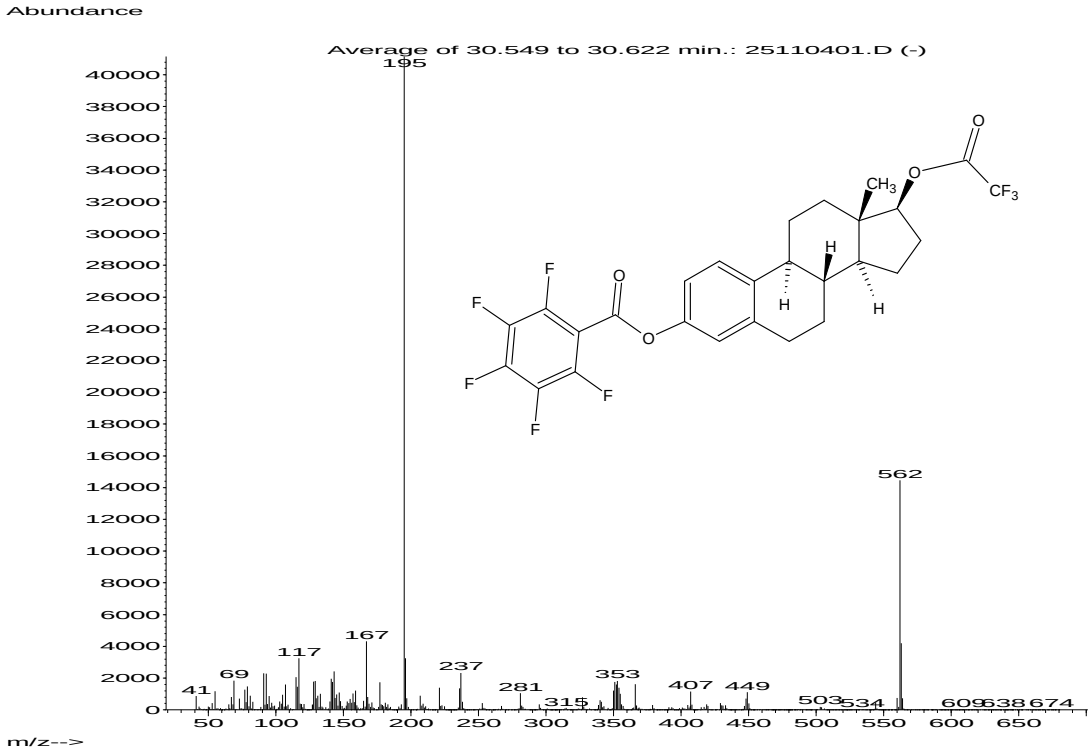


**Figure 6.19 The EI Mass Spectrum obtained for the derivative formed from the reaction of 17β-Estradiol (E2) with PFBCl and TFAA. Base peak m/z 195 ($C_7F_5O$), m/z 69 ($CF_3$) and $M^+$ m/z 562.**

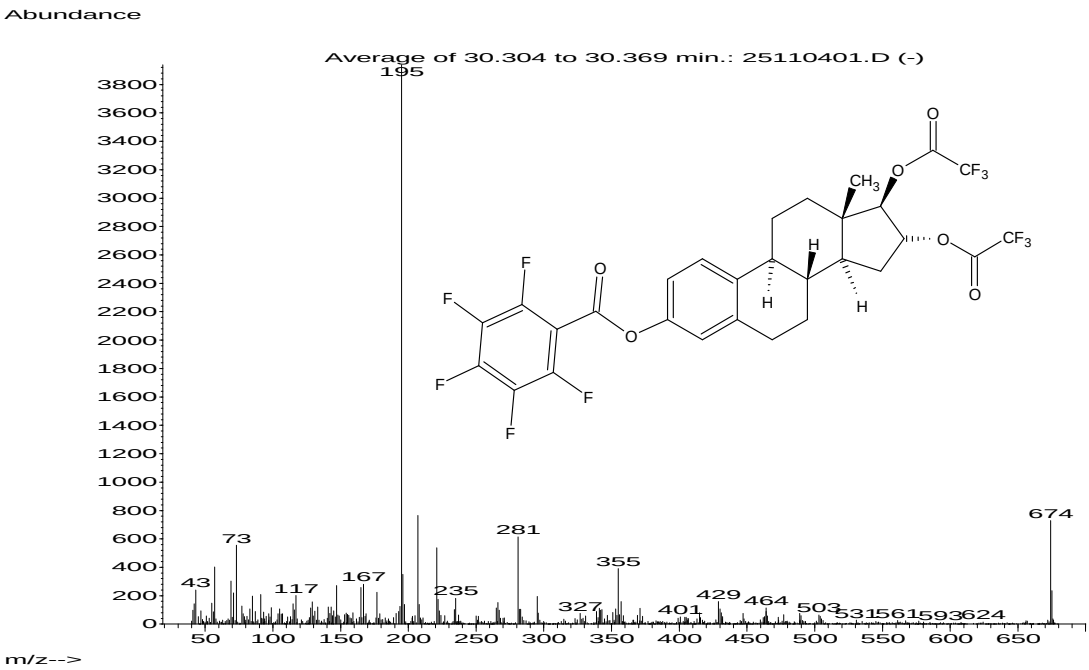


**Figure 6.20 The EI mass spectrum obtained for the derivative formed from the reaction of estriol (E3) with PFBCl and TFAA. Base peak m/z 195 ($C_7F_5O$), m/z 69 ($CF_3$) and $M^+$ m/z 674.**

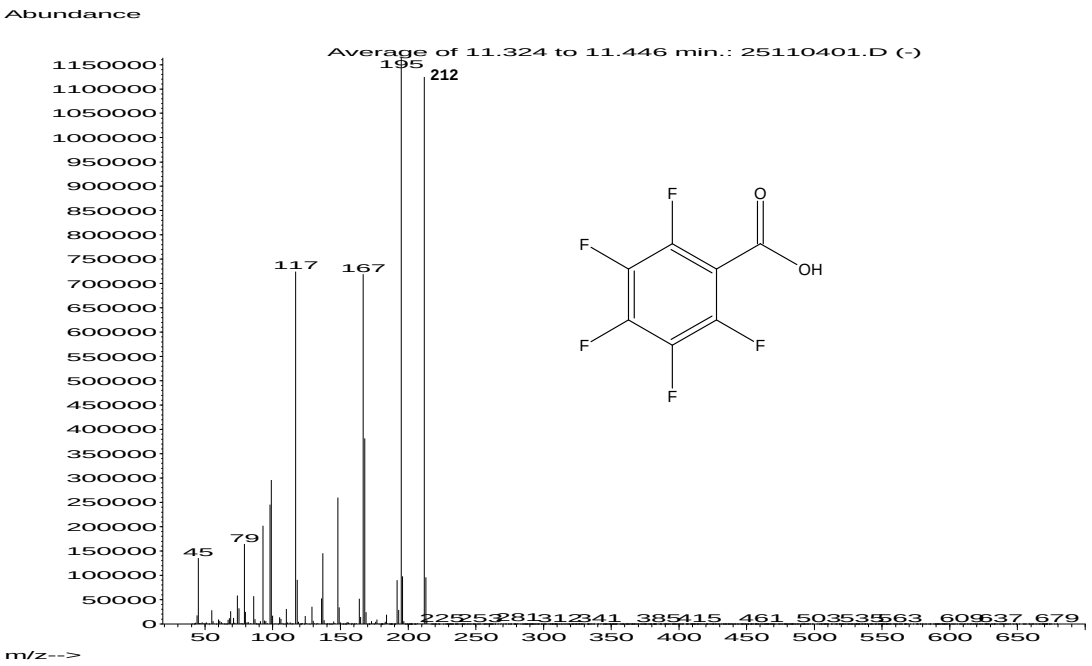


**Figure 6.21 The EI mass spectrum obtained for the hydrolysed PFBCl, i.e. Pentafluorobenzoic acid formed from the reaction of the estrogens with PFBCl and TFAA. Base peak m/z 195 ($C_7F_5O$), and $M^+$ m/z 212.**

## *6.2.5. Reagent selection for the alkylphenols*

From chapter 3, it is clear that acylation with acetic acid anhydride (AAA), prior to extraction, is the preferred derivatization reaction for phenols. The reaction is favoured because it does not require anhydrous reaction conditions and proceeds easily, even in aqueous media. Table 3.2 summarises what has been achieved with other sorptive devices, such as SBSE and SPME using AAA.

In order to decrease the detection limits for the alkylphenols and bisphenol-A, it was decided to form an electron-capturing halogenated derivative suitable for analysis by GC/ECD and GC/NCI-MS. The reaction should proceed with the same ease as for acetic acid anhydride. Trifluoroacetic acid anhydride reacts rapidly with phenols to form the stable trifluoroacetate derivative and trifluoroacetic acid [62]. The reaction mechanism is shown below in figure 6.22. The nucleophilic oxygen on the phenol attacks the electrophilic carbon on the TFA acid anhydride. The trifluoroacetate ion then abstracts a proton to form TFA acid and the corresponding TFA ester. Ordinarily, the acid by-product is removed before instrumental analysis, as the acid would destroy the chromatographic column. The volatile TFA acid however, elutes at low temperatures and does not require prior removal, unlike its related perfluoroacyl anhydrides, PFPAA and HFBAA [250].

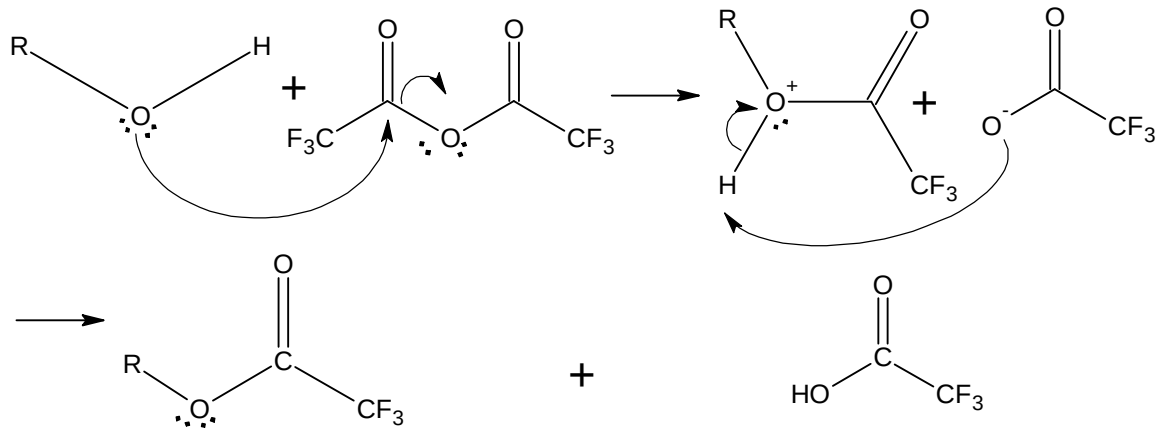


**Figure 6.22 Reaction mechanism for the derivatization of a primary alcohol with trifluoroacetic acid anhydride (TFAA) to form the corresponding trifluoroacetate derivative and trifluoroacetic acid by-product.**

## *6.2.6. Derivative confirmation*

The trifluoroacetate (TFA) derivatives of TOP, NP and BPA were prepared in acetone using the simple method described by Lerch and Zinn [62]. 10 µl TFAA is added to the alkylphenol standard in acetone and allowed to react; after 5 min the reaction is complete. An aliquot from this reaction mixture is injected. The synthesized derivative was used for comparison and as an external standard to quantitate the TFA derivatives formed *in situ* in the PDMS traps. Refer to appendix 3 for confirmation chromatograms of the acetone synthesized derivatives.

The electron impact mass spectra, obtained under GC-EI-MS conditions given in section 6.6.1, for each derivative formed is shown below, along with the main fragment formation mechanism. Typically molecular ions of phenyl esters eliminate the neutral ketene after the hydrogen/ atom X on the terminal $CX_3$ group is transferred to the ether oxygen and the ether oxygen-carbon bond is cleaved (see figure 6.23 and figure 6.24). This is not the case for the trifluoroacetate esters, as the electron rich fluorine atom does not migrate to the ether oxygen. Instead, alpha cleavage at the alkyl chain is observed [62, 251, 252]. The bisphenol-A derivative loses a $CH_3$ radical to form the abundant base peak m/z 405 [62, 252] (see figure 6.25). Another advantage of the TFA esters is that the most abundant fragments fall in a higher mass range than their corresponding acetate esters.

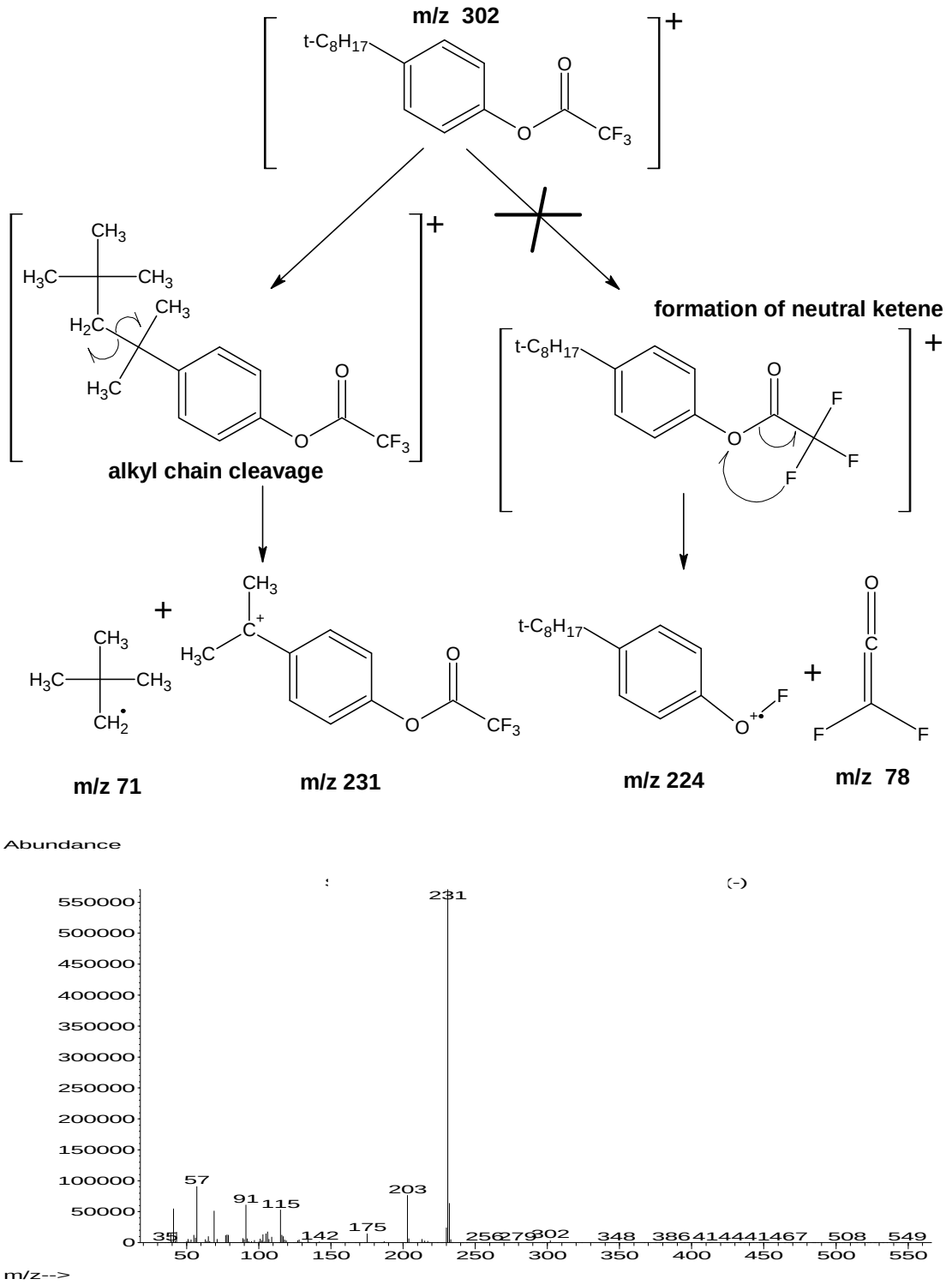


**Figure 6.23 Mass spectrum and fragmentation scheme for the main mass spectral fragments obtained for the *tert*-octylphenol TFA derivative. Note the molecular ion (m/z 302) is almost absent.**

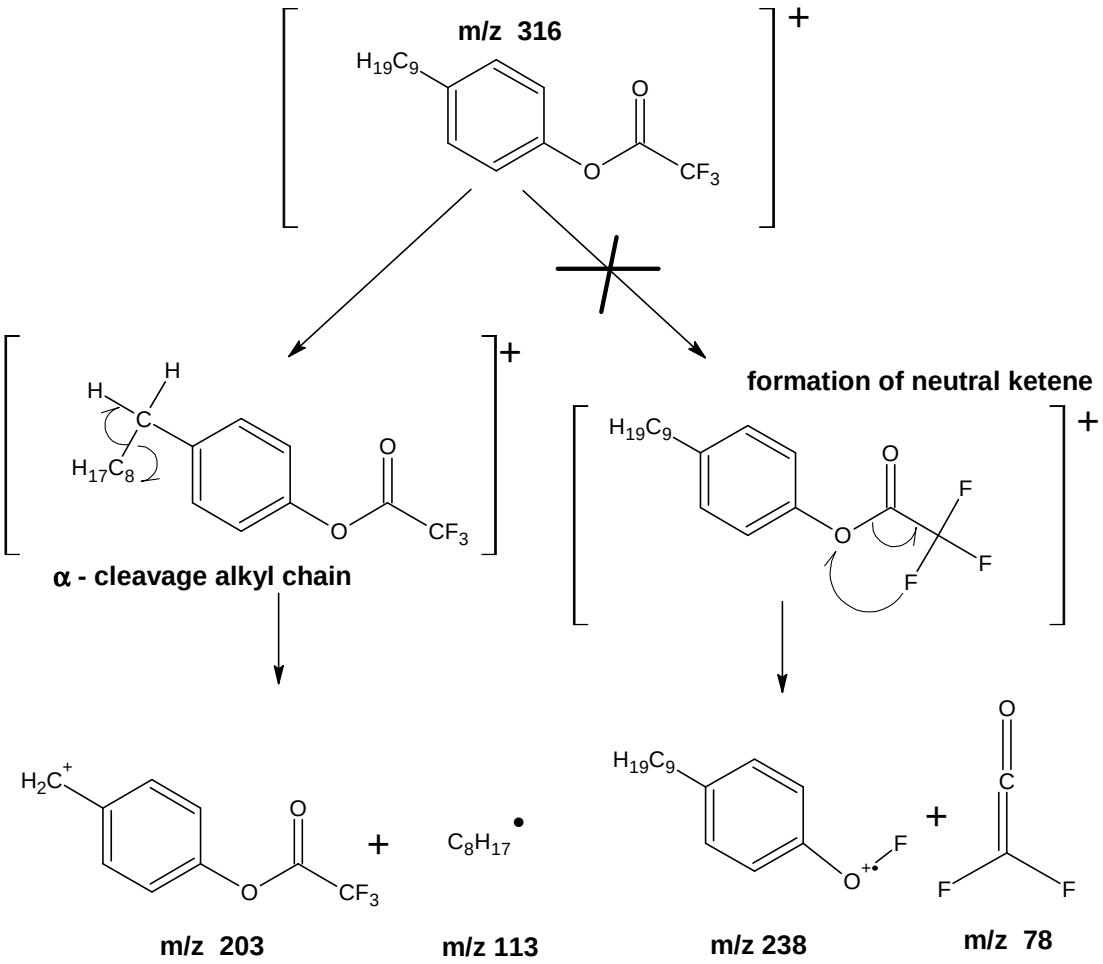


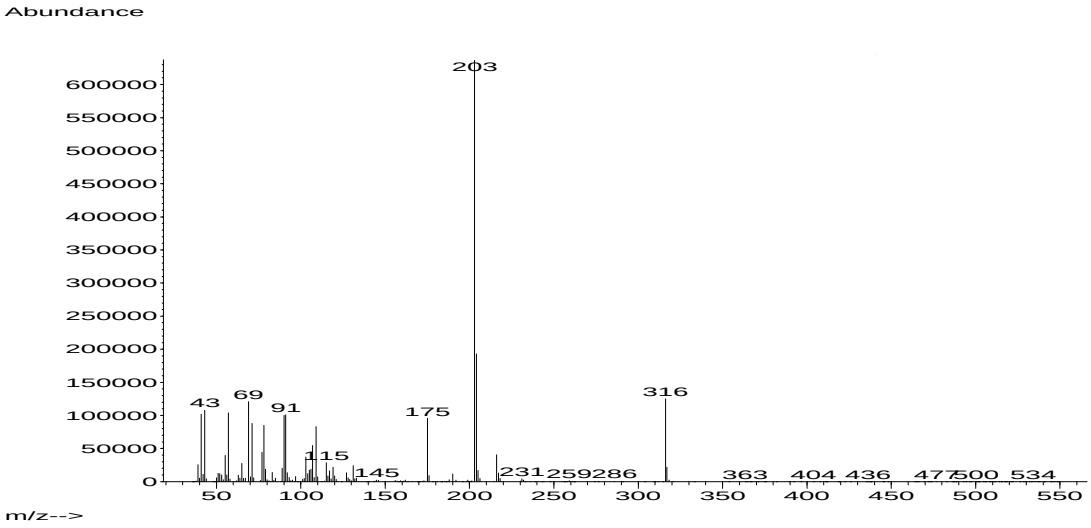


**Figure 6.24 Mass spectrum and fragmentation scheme for the main mass spectral fragments obtained for the 4-*n*-nonylphenol TFA derivative.**

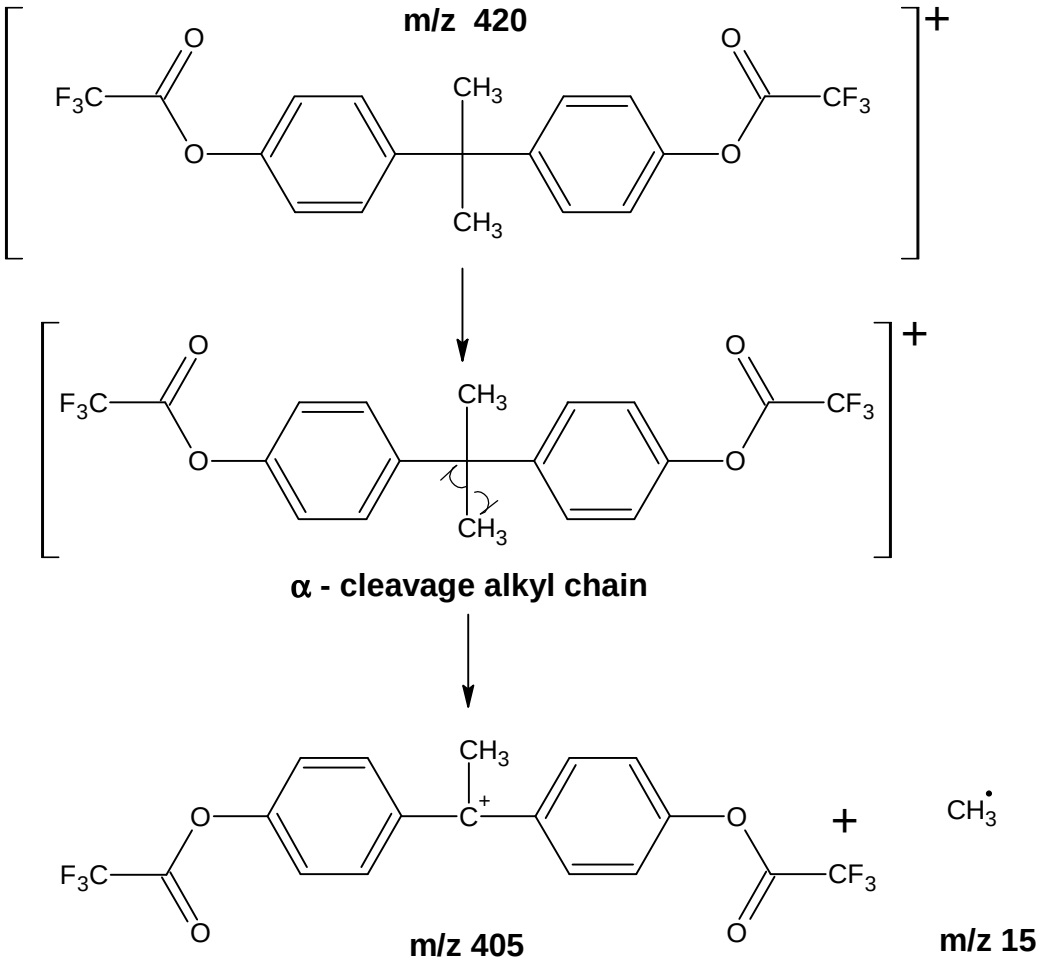


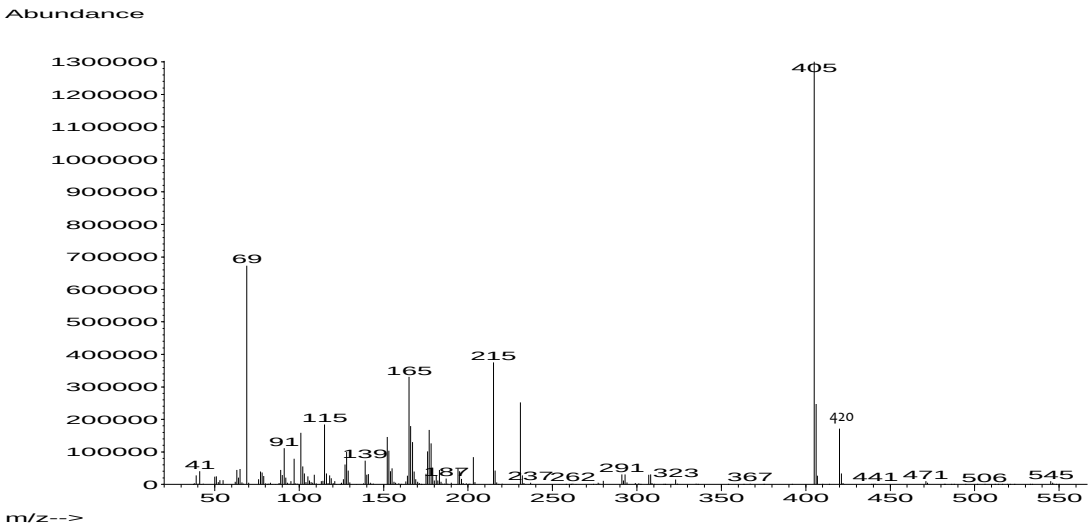


**Figure 6.25 Mass spectrum and fragmentation scheme for the main mass spectral fragments obtained for the bisphenol-A TFA derivative.**

## 6.3. Extraction

### 6.3.1. Predictions based on $K_{o/w}$

Initial calculations to predict the extraction efficiency of the estrogens and alkylphenols (defined in table 6.1) were determined using the phase ratios of the PDMS concentration devices, octanol – water partition coefficients ($K_{O/W}$) for the analytes and equation 2.3 (see chapter 2 section 2.5, page 39). Naturally equation 2.3 is for static equilibrium sampling techniques such as SPME and SBSE. However, as discussed in section 2.4.5 (page 38), dynamic equilibrium sampling (post-breakthrough volumes) should yield similar recoveries. Dynamic equilibrium sampling can be considered the "worst-case scenario" where full breakthrough of all analytes off the trap has occurred and complete equilibrium is reached. It is only appropriate if neither sample volume nor sampling time are not restricted. Predicted recoveries are shown in table 6.3.

$$\frac{m_{PDMS}}{m_0} = \frac{\left(\frac{K_{O/W}}{\beta}\right)}{1+\left(\frac{K_{O/W}}{\beta}\right)} \qquad (2.3)$$

**Table 6.3 Prediction of analyte recoveries on 3 different PDMS devices, using equation 2.3.**

| Analyte | Log $K_{O/W}$ * | % Recovery from a 10 ml water sample | | |
|---|---|---|---|---|
| | | MCT (β = 40) | SBSE (β = 100) | SPME (β = 20000) |
| 17α-ethinylestradiol | 4.42 | 99.96 | 99.62 | 56.98 |
| 17β-estradiol | 4.48 | 99.96 | 99.67 | 60.27 |
| estriol | 3.50 | 99.65 | 96.94 | 13.68 |
| estrone | 4.40 | 99.96 | 99.60 | 55.39 |
| testosterone | 3.77 | 99.81 | 98.31 | 22.54 |
| *tert*-octylphenol | 4.54 | 99.88 | 99.71 | 63.37 |
| 4-*n*-nonylphenol | 5.46 | 99.99 | 99.96 | 93.44 |
| bisphenol-A | 3.84 | 99.43 | 98.58 | 25.79 |

* Values obtained from http://www.molinspiration.com/cgi-bin/properties (date: 20 August 2006)

Based on the values presented in table 6.3, it is expected that the analytes will partition very well into the PDMS MCT, without requiring derivatization prior to extraction. Since we did not intend to perform dynamic equilibrium sampling, as this will require extended sampling periods of time, typical retention volumes that could be expected for these analytes on the PDMS MCT by dynamic breakthrough sampling were calculated. This was achieved using Baltussen's equations for aqueous phase dynamic sampling (section 2.4.4 page 37) in determining retention volumes (equation 2.20) and breakthrough volumes (equation 2.21) for a trap.

$$V_r = V_0\left(1+\frac{K_{O/W}}{\beta}\right) \tag{2.20}$$

$$V_b = V_r\left(0.9025+\frac{5.360}{N}+\frac{4.603}{N^2}\right)^{-1/2} \tag{2.21}$$

Table 6.4 shows how the parameters for the PDMS MCT are calculated from geometric considerations. The value for the number of plates is hypothetical for these analytes, and was taken from reference 63 i.e., determined experimentally for benzene on a 32 MCT with similar dimension and flow rate.

**Table 6.4. Geometrically calculated parameters for the PDMS MCT.**

| *Parameters for the PDMS MCT:* | |
|---|---|
| No. of PDMS tubes | 32 |
| Length (L) (cm) | 5 |
| i.d (cm) / i.r (cm) | 0.03 / 0.015 |
| o.d (cm) / o.r (cm) | 0.065 / 0.0325 |
| Volume of 1 tube (ml) = L [ $\pi r^2$ (o.d) - $\pi r^2$ (i.d) ] | 0.013 |
| Volume of total tube no. (ml) | 0.417 |
| Subtract 40 % ($SiO_2$ filler contribution) (ml) | 0.167 |
| Volume PDMS (ml) | 0.250 |
| Volume sample (ml) | 10 |
| Phase ratio β | 40 |
| Glass trap tube i.d (cm) / i.r (cm) | 0.4 / 0.2 |
| Volume glass trap tube = L [ $\pi r^2$ ] | 0.628 |
| Void Volume $V_0$ = Volume (glass tube – PDMS) | 0.211 |
| No. of theoretical plates N | 11 |

**Table 6.5 Predicted retention ($V_r$) and breakthrough volumes ($V_b$) for analytes on the PDMS MCT.**

| *Analytes* | Log $K_{O/W}$ * | $K_{O/W}$ | $V_r$ (ml) | $V_b$ (ml) |
|---|---|---|---|---|
| *tert*-octylphenol | 4.54 | 34 594 | 183 | 153 |
| 4-*n*-nonylphenol | 5.46 | 285 102 | 1 505 | 1 259 |
| bisphenol-A | 3.84 | 6 950 | 37 | 31 |

For dynamic pre-breakthrough sampling of aqueous analytes through the MCT, table 6.5 predicts that 4-*n*-nonylphenol will have the best retention (1 ½ L) followed by *tert*-octylphenol (180 ml). Bisphenol-A exhibits the poorest retention (37 ml). Breakthrough volumes were calculated at the 5% level. Once mass detection limits are determined, the sample volume can be selected within the required breakthrough volume for that analyte.

### *6.3.2. pH adjustments*

Extraction into the PDMS matrix is based on the octanol-water partition coefficients ($K_{o/w}$) of the neutral analytes, since it is already known that analytes in their ionic form will remain in the aqueous phase. The phenolic analytes are weak acids which have $pK_a$s well above 10 indicating that they will remain in their non-ionized form at typical environmental pHs [7], although a pH of 7 or less is preferred, to ensure protonation of the weak acids.

In greater detail the influence of $pK_a$ on partitioning can be expressed as follows [253]. The total analyte concentration ratio between the organic and aqueous phases is described by the distribution ratio $D_c$ denoted by:

$$D_c = \frac{[analyte]_{organic}}{[analyte]_{aqueous}} \qquad (6.1)$$

The partitioning between the 2 phases is described by the partitioning constant $K_p$ or as in our case $K_{o/w}$:

$$K_p = \frac{[HA]_{organic}}{[HA]_{aqueous}} \approx K_{o/w} \qquad (6.2)$$

The acid dissociation constant $K_a$ describes the dissociation of an acid in water (aqueous phase):

$$K_a = \frac{[H^+]_{aqueous}[A^-]_{aqueous}}{[HA]_{aqueous}} \quad (6.3)$$

Assuming that ions are not soluble in the organic phase, $D_c$ can be rewritten to give:

$$D_c = \frac{[HA]_{organic}}{[HA]_{aqueous} + [A^-]_{aqueous}} \quad (6.4)$$

*The total concentration of analyte in the aqueous phase is the amount of acid plus the amount of acid that dissociates.*

Equation 6.2, 6.3 and 6.4 are combined to yield the following:

$$D_c = \frac{[HA]_{organic}}{\frac{[HA]_{organic}}{K_p} + \frac{K_a}{K_p}\frac{[HA]_{organic}}{[H^+]_{aqueous}}} \quad (6.5)$$

Equation 6.5 simplifies to:

$$D_c = \frac{K_p[H^+]_{aqueous}}{[H^+]_{aqueous} + K_a} \quad (6.6)$$

If $K_a$ is much larger than [H+] then:

$$D_c = \frac{K_p[H^+]_{aqueous}}{K_a} \quad (6.7)$$

And if [H+] is much larger than $K_a$ then:

$$D_c = K_p \quad (6.8)$$

The pH of all aqueous samples analysed was determined using universal pH paper. The pH of all samples was in the range of 5-6, including the MilliQ water blanks. No pH adjustments were therefore necessary. The ionization of these analytes analysed from water are depicted in table 6.6, along with their associated $pK_a$ values [254]. The estrogens are not shown in this table, but their pKa's are also above 10 [21] as well. For these conditions the acid remains largely non-ionized (from equation 6.3):

$$\frac{[A^-]_{aqueous}}{[HA]_{aqueous}} = \frac{K_a}{[H^+]_{aqueous}} = \frac{10^{-10}}{10^{-6}} = 10^{-4}$$

In addition, the distribution coefficient for a $pK_a$ of 10 and pH of 6 ($K_a = 10^{-10}$ and $[H^+] = 10^{-6}$; $[H^+] >> K_a$) amounts to $K_{o/w}$ (equation 6.8) as described by equation 6.2.

**Table 6.6 Structure of the alkylphenols and bisphenol-A as they ionize in aqueous medium plus their associated ionization constants at 25ºC [7, 254].**

| *Analyte ionization in water* | *pKa* | *Ka* |
|---|---|---|
| 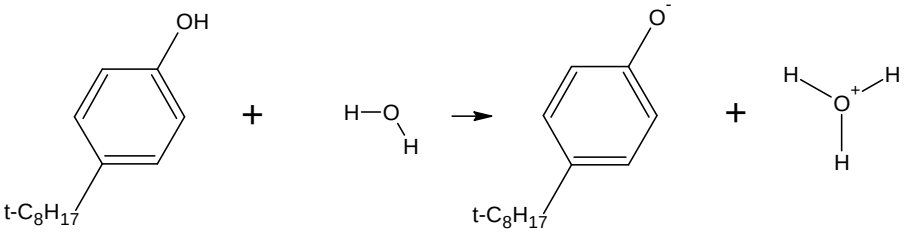 *tert*-octylphenol | 10.25 | $5.62 \times 10^{-11}$ |
| 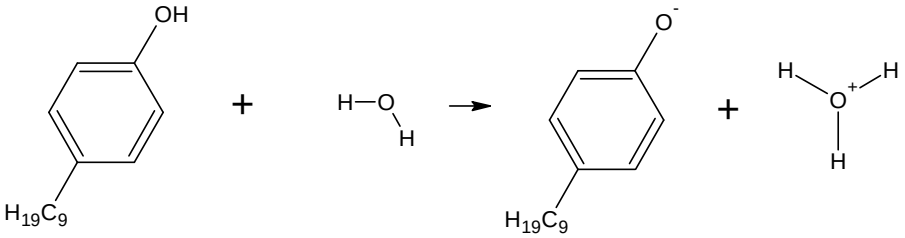 4-*n*-nonylphenol | 10.28 | $5.25 \times 10^{-11}$ |
| 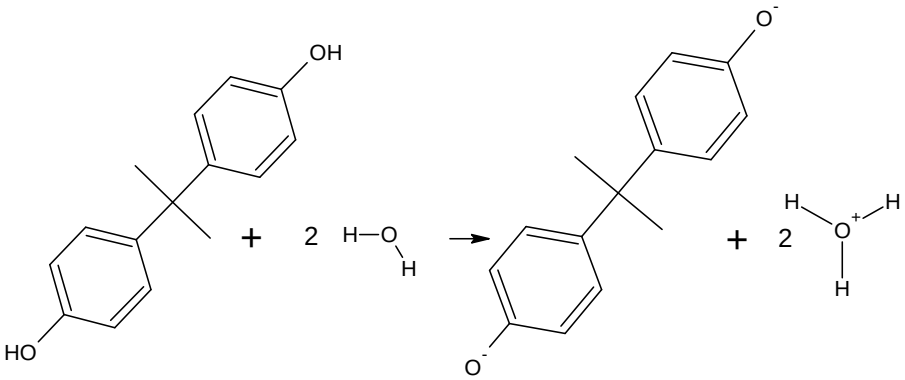 bisphenol-A | 9.5<br>11.3 | $3.16 \times 10^{-10}$<br>$5.01 \times 10^{-12}$ |

## 6.4. Quantitative Thermal Desorption

### 6.4.1. Optimising desorption conditions

Several experiments were performed to determine the conditions under which the derivatives would be completely transferred to the GC column i.e. when desorption is complete. As described in chapter 2, the MCT can be compared to a chromatographic column having a PDMS stationary phase. Compounds will elute off the MCT in the same order as compounds elute off a non-polar (PDMS stationary phase) GC column.

Based on previous work in my MSc thesis [61], concerning thermal desorption optimisation, it is convenient to optimise conditions using the alkane that elutes after the analyte of interest. Nonadecane (C19) is the alkane eluting immediately after the BPA-TFA derivative on a PDMS phase GC column. However, several alkanes with increasing boiling points (hence elution temperatures) were used, since this would be useful for future applications. Little additional effort was required to include them. The alkanes selected were C16, C20, C24 and C28. These were placed at the top of the PDMS MCT using a 5 µL syringe. As desorption flow is from the top to the bottom of the trap, once the alkanes are completely desorbed it is evident that any compound that elutes before that specific alkane on a PDMS phase GC column, has also been completely desorbed from the PDMS MCT. Traps were analysed using the Gerstel ® TDS-CIS HP GC-FID instruments.

Figure 6.26 shows a graph of the various alkane FID peak areas *versus* desorption temperature, for TDS desorption time of 20 minutes, desorption flow rate of 100 ml/min, and CIS injection time of 20 min at 300ºC, with a reduced injection flow rate of 5 ml/min. The capillary column limits the CIS injection flow rate. Figure 6.27 shows that more than 10 minutes are required to desorb the alkanes from the CIS at 300ºC, as a result of the lower flow rate available for this process. As shown in figure 6.26 all the alkanes have reached a maximum peak area from 180ºC onwards. It can be concluded that they have all been completely transferred from the PDMS trap. A temperature of 260ºC was chosen for the desorption process, as it was later learned that desorption flow rates greater than 50 ml/min through a glass baffled inlet liner may cause incomplete trapping in the CIS. This is half the flow rate used during desorption temperature

optimisation. A temperature of 260ºC also ensured that other non-interesting compounds on the trap would be desorbed. Silicone degradation increases with higher temperatures, which result in increased silicone peak areas (section 2.6), causing additional problems such as peak overlap, column overload and contamination of the MS ion source. For this reason higher temperatures were not chosen. A blank run of the PDMS MCT after this desorption cycle indicated complete transfer of the derivatives and C19; no carry-over was observed. C19 was added, as an internal standard, to all traps just before desorption in the Gerstel ® unit. The C19 was used only to check for losses in the desorption unit during the desorption process.

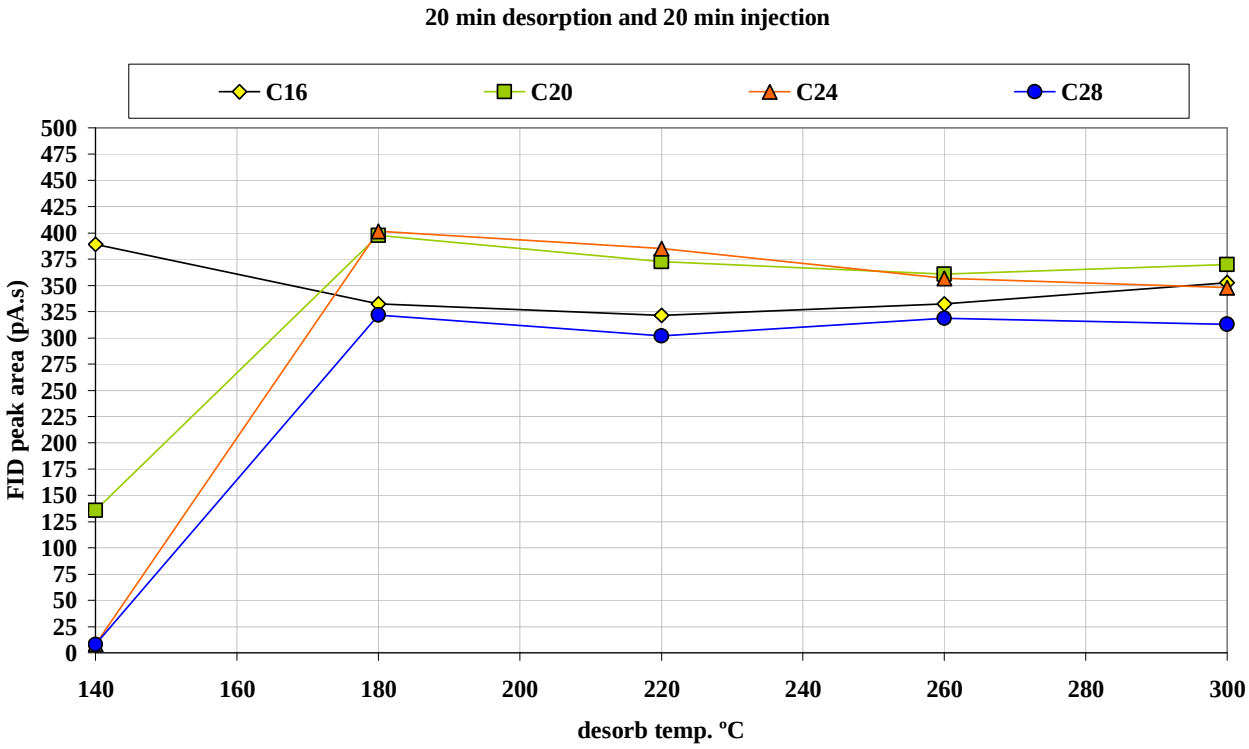


**Figure 6.26 Optimisation of thermal desorption temperature of higher boiling alkanes off a 32 PDMS MCT using a Gerstel® TDS-CIS. The injection temperature was maintained at 300ºC, while desorption temperature was incremented by 40ºC per desorption run. The measurement values are depicted as an x-y scatter plot with data points connected by lines. The optimum desorption temperature was visually determined to be 180ºC where the peak areas of the analytes appear to reach a plateau.**

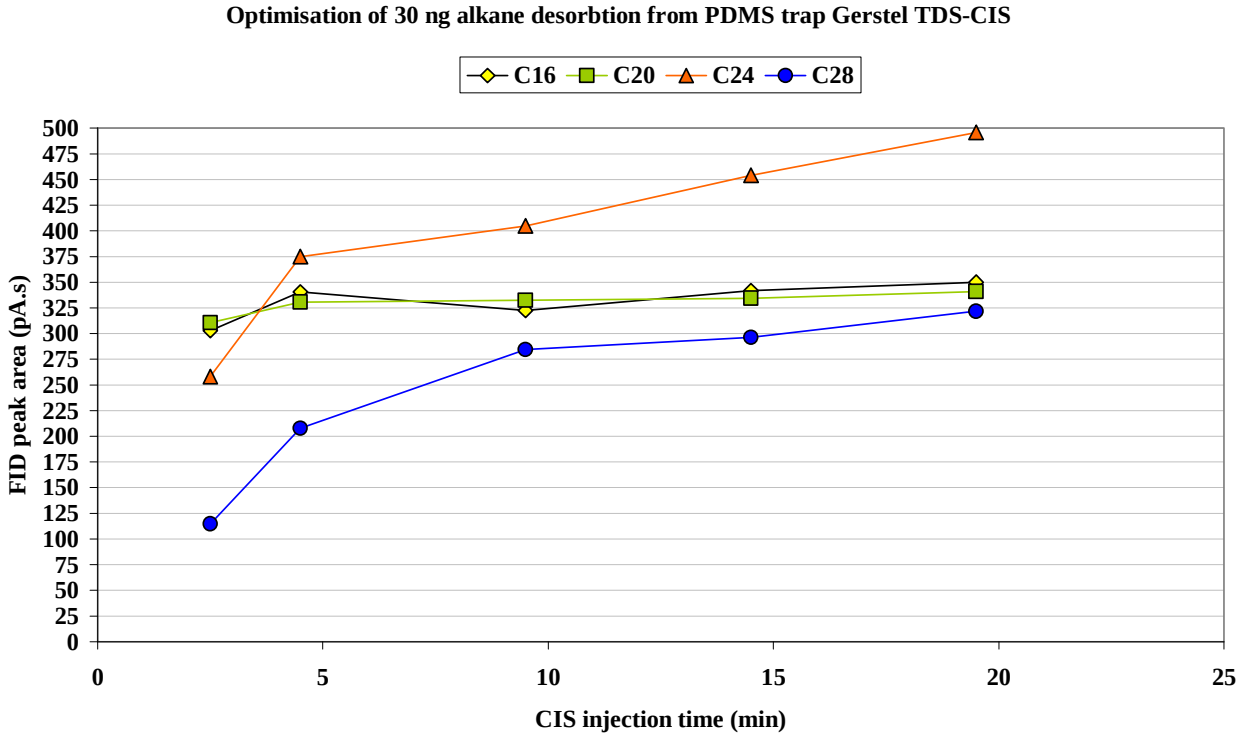


**Figure 6.27 Optimisation of CIS injection time of higher boiling alkanes off a glass baffled inlet liner using a Gerstel® TDS-CIS at 300ºC. The measurement values are depicted as an x-y scatter plot with data points connected by lines. The optimum CIS injection time was visually determined to be 5 min for alkanes from C16 to C20, as the peak areas of these analytes appear to reach a plateau at this time. Higher boiling alkanes (C24 to C28) require more than 20 minutes to be desorbed completely off the CIS. A midpoint of 10 min was selected for injection time in this study.**

### *6.4.2. The "Christmas tree effect"*

During thermal desorption the excess derivatization reagent, derivatives and by-product, as well as the PDMS thermal degradation products, are injected onto the GC column. Under ideal conditions, the solvent forms a homogenous film that wets the stationary phase allowing the analytes to partition into the phase and begin the chromatographic process, producing the standard Gaussian chromatographic peaks, figure 6.28 (A). This only occurs if the polarities of the solvent and stationary phase are matched. In our case, however, the TFAA and TFA are polar solvents, which are present in a quantity that exceeds 1-2µl. Thus, instead of forming a homogenous wetting film on the PDMS stationary phase, droplets are formed inside the column. Each droplet gives rise to its own "solvent effect" i.e. analytes partition into the PDMS once the droplet of solvent has evaporated. This can occur at various points along the column. As a result the peaks that elute are

no longer gaussian but broader "Christmas tree-like" peaks, figure 6.28 (B). This is a typical occurrence in large volume splitless injections, and the problem can normally be overcome by inserting a retention gap before the GC column [255]. In our study an alternative to the retention gap is suggested. This is made possible through the use of a PTV injector or CIS in this case.

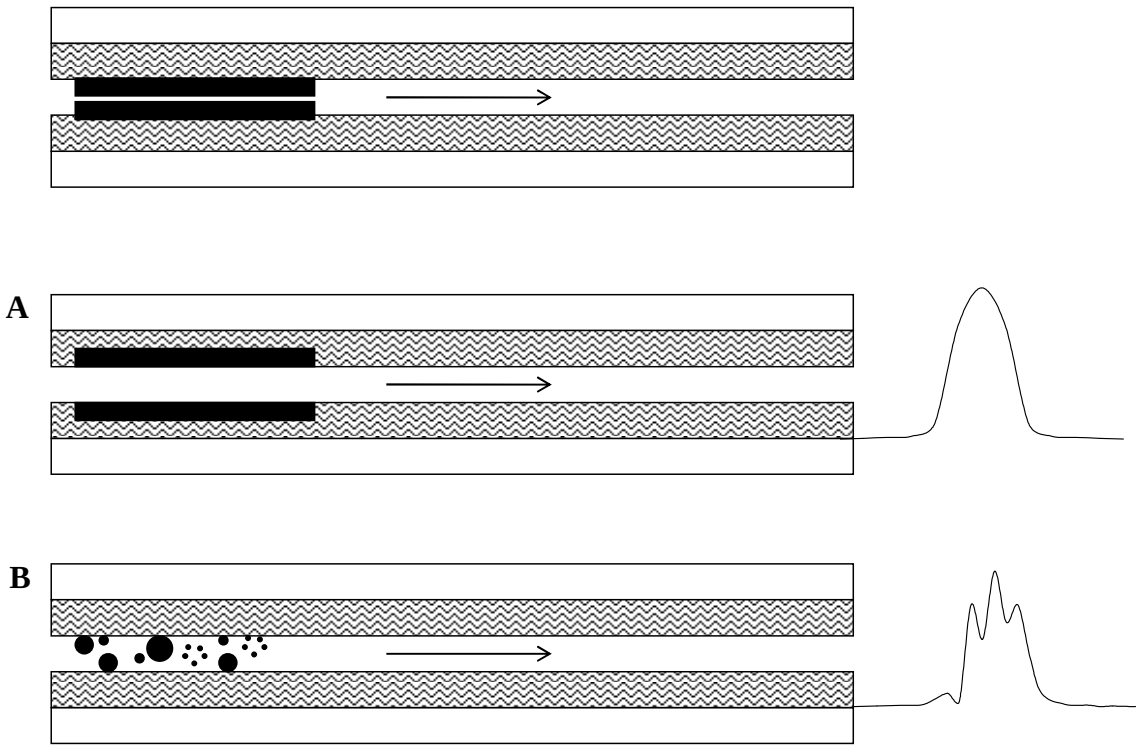


**Figure 6.28 Cross-section of a non-polar capillary column showing a large volume splitless injection using (A) a non-polar solvent and (B) a polar solvent. The top figure shows the injection plug entering the column in the mobile phase. Figure A shows how the non-polar solvent "wets" the stationary phase as "like-dissolves-like". The analytes in the plug begin to partition into the stationary phase and start the chromatographic process resulting in Gaussian peaks eluting from the column. Figure B shows how the polar solvent forms droplets as it does not wet the stationary phase. Each droplet gives rise to its own solvent effect resulting in broad split peaks eluting from the column [255].**

Initial injection conditions from the cooled inlet onto the GC column were as follows:
The CIS is ballistically heated from -100ºC to 260ºC where it is held for 20 min, while the analytes move onto the column, then held at 40ºC for 20 min, at an approximate flow rate of 5 ml/min. Since the TFA can cause damage to the column at higher temperatures the aim is to remove it prior to raising the column temperature. However, this should not be at the expense of creating "Christmas trees". By altering the injection conditions so that the solvent is selectively desorbed

(based on boiling point) from the CIS prior to desorption of the analytes, it is possible to remove the excess TFA such that the "Christmas tree" effect is avoided.

The CIS desorption conditions were altered as follows:
The CIS was heated from -100ºC to 35ºC, where it was maintained for 10 min. During this period, the TFA moved off the CIS onto the column. However, since the column was maintained at 40ºC for 20 min, the "solvent" could not recondense, but moved straight through the column unretained. At this point the CIS was heated to 260ºC and held for 10 min, while the analytes were focussed onto the column at 40ºC. Figure 6.29 shows a section of two overlaid chromatograms indicating the improvement in chromatography as a result of the changed injection parameters.

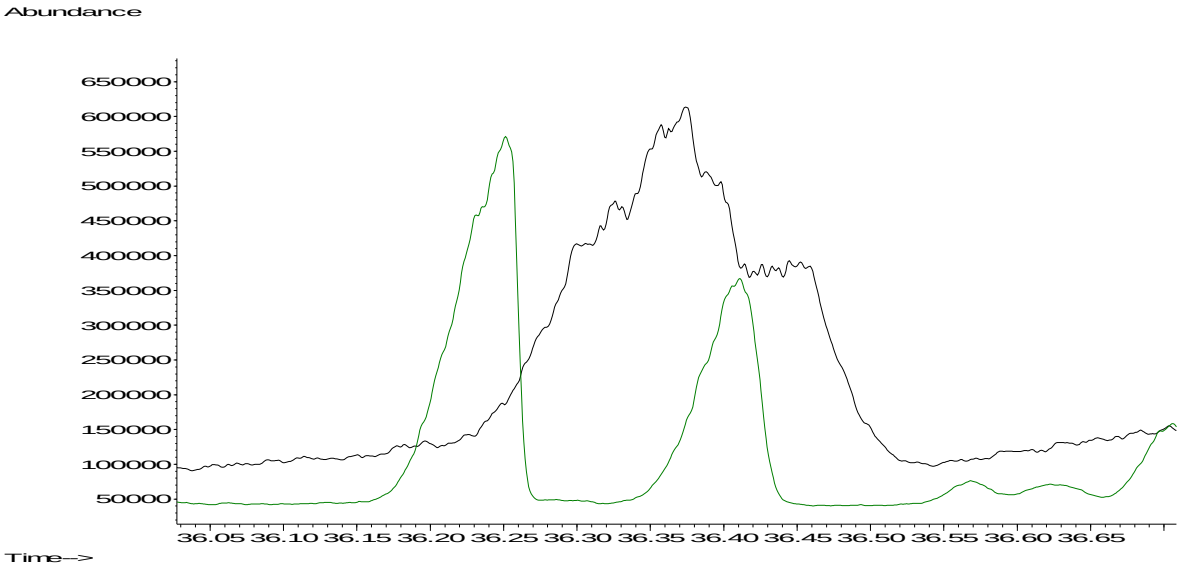


**Figure 6.29 Section of two overlaid chromatograms depicting the improvement of chromatographic conditions for a large volume splitless injection. The "Christmas tree effect" of the larger co-eluting peak is replaced by 2 separated, smooth, peaks.**

## *6.5. Sampling*

### *6.5.1. Sampling setup and procedure*

Figure 6.30 shows the simple setup used for sampling water through the PDMS MCT in the lab. A glass funnel was used as the water sample reservoir at the top of the PDMS MCT. It was connected to the MCT via a piece of Teflon® tubing. At the outlet of the MCT, a length of fused silica capillary was again connected with Teflon® tubing (fitted in a Swagelok ® reducing union ¼" to

1/16") which acted as a flow restrictor. By adjusting the height of the restrictor outlet relative to the height of the water sample meniscus, (i.e. the pressure drop), it was possible to regulate the flow rate through the trap. Similar flow rates through the MCT could be obtained for all sampling arrangements using this setup. A sampling flow rate of approximately 50 µl/min was used throughout this study. Based on previous work by Ortner, 11 plates can be obtained on the 32 channel PDMS MCT at 75 µl/min for benzene in aqueous samples [63].

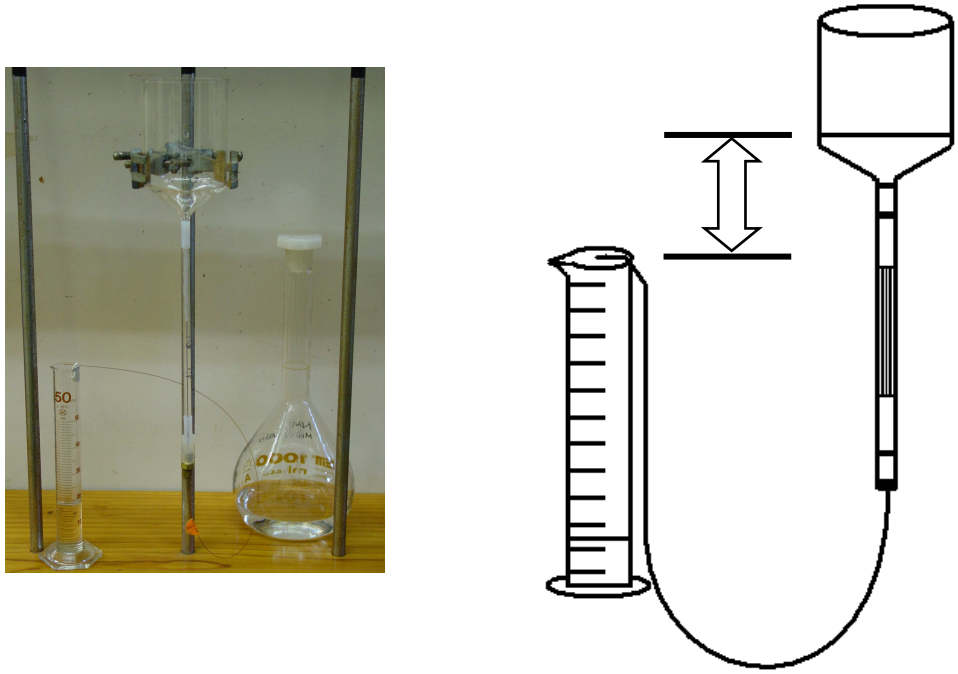

**Figure 6.30 The simple setup used in the lab to sample water through the PDMS MCT.**

The PDMS MCT trap must be conditioned with water before sampling, to ensure that no air bubbles are present as this affects the sampling flow rate through the channels in the trap. From Henry's Law for gases [256] we know that the solubility of a gas is inversely related to the temperature of the solvent, i.e. the warmer the solvent the less gas is dissolved in it. Thus pouring water at a temperature of approximately 60ºC, through the trap was sufficient to remove any air bubbles that formed in the process. Tapping the PDMS MCT with a rubber tube during the conditioning step decreased the time required for degassing the trap. The water was allowed to reach just above the start of the PDMS at which point the sample was added. The water sample could only be added to the PDMS MCT once the trap had reached room temperature again. A Pasteur pipette was used to suck out the bubble that formed in between the two water levels.

The risk of losing analytes through adsorption onto active sites on the glassware was possible at this stage. It was assumed that the amount of time that the sample spent in the sampling funnel was short enough such that adsorption would not occur. Usually an organic modifier such as methanol could be added to the sample to prevent adsorption from occurring [47].

## *6.6. Experimental*

### *6.6.1. Instrumentation*

The analyses were performed on an Agilent 6890 GC system equipped with an FID or a 5973 Mass Selective Detector (Agilent Technologies, Palo Alto, CA, U.S.A) coupled to a Gerstel TDS-CIS4 thermal desorption unit (Gerstel, Mülheim an der Ruhr, Germany). An empty glass-baffled inlet liner was fitted in the CIS4; liquid nitrogen was used as the cryogen.

The thermal desorption conditions were as follows:
Desorption temperature 260ºC; desorption time 20 min; helium desorption flow rate 50 ml/min (solvent vent mode); transfer line temperature 280ºC.

The cold inlet conditions were as follows:
CIS trap temperature during thermal desorption -100ºC; inject splitless for 10 min; 1$^{st}$ heating rate 10ºC/s, initial injection temperature 35ºC hold time 5 min, 2$^{nd}$ heating rate 10ºC/s, final injection temperature 280ºC hold time 5 min.

The GC oven was fitted with an HP-5 capillary column (30 m length, 0.25 mm i.d. and 0.25 µm film thickness). The oven was programmed as follows: 40ºC (hold for 10 min during the splitless injection) to 160ºC at a rate of 12ºC/min (hold 3 min) and to 220ºC at a rate of 12ºC/min. The oven was then heated to 300ºC (hold for 2 min). Helium was used as carrier gas with an average linear velocity of 40 cm/s. The FID temperature was set to 300ºC. The GC-MSD transfer line was set to 280ºC.
The MSD was programmed either for total ion scan from 40-500 amu or for SIM: m/z 231, 203, 245, 216, 405, 420, the 3 most abundant ions for each derivative.

### 6.6.2. Reagents and Materials

Trifluoroacetic acid anhydride (TFAA) was obtained from Supelco (Bellefonte, U.S.A.), 4-*tert*-octylphenol (TOP) from Aldrich (Steinheim, Germany), 4-*n*-nonylphenol (NP) from Riedel-de Haën (Steinheim, Germany) and bisphenol A (BPA) from Fluka (Steinheim, Germany). Medical grade PDMS tubing was obtained from Sil-Tech technical products (Georgia, USA). The method adopted for preparing PDMS MCTs is described in the literature [65].

### 6.6.3. Extraction Efficiency

2 ml MilliQ water was spiked with 1 µl of a 40 ng/µl solution of alkylphenols and bisphenol-A in methanol. The water was sampled by pouring it through a funnel connected to the PDMS trap with Teflon® tubing. The flow through the trap was regulated using a capillary restrictor connected at the PDMS trap outlet. The sampling flow rate was set at approximately 50 µl/min. After sampling, residual water was removed by physically tapping it out, then purging (1 minute) with a fast stream (approximately 1 L/min) of hydrogen gas introduced through a capillary. The traps were then plugged with silica gel to remove any further water vapour before derivatization. The silica gel was baked in an oven at 100ºC when not in use. The plugs were prepared using glass tubes of the same dimension as the PDMS MCT. Each tube has one side sealed off. The silica gel is packed into the tube which is then pressed onto the PDMS trap using a tightly fitting Teflon® sleeve. The silica gel does not come into physical contact with the PDMS. No signs of contamination originating from this operation was observed in the resulting chromatograms. Recoveries were compared to a 40 ng standard in acetone, placed on the PDMS trap, reacted and desorbed.

This extraction efficiency experiment was repeated twice. The first series of extractions was performed using a set of traps prepared from the same batch of silicone. The extracted analytes from this first set of traps were analysed by GC-FID. The second series of extractions was performed using a set of traps prepared from a different batch of silicone to the first series. The extracted analytes from these traps were analysed by GC-MS (using reconstructed ions).

### 6.6.4. Reaction efficiency

The optimum reagent volume was determined by placing 1 µl of a 40 ng/µl alkylphenol standard in acetone onto the PDMS and allowing the acetone to evaporate. Different volumes ranging from 2 µl to 10 µl of TFAA was added using a 10 µl syringe. The trap was capped on both ends with glass plugs for 10 minutes.

The reaction efficiency was tested by placing 1 µl of a 40 ng/µl alkylphenol standard in acetone onto the PDMS and allowing it to evaporate. 5 µl TFAA was added using a 10 µl syringe. The trap was capped on both ends with glass plugs for the duration of the reaction. This experiment was repeated for different reaction times. Structures of the derivatives were confirmed by EI mass spectrometry (figure 6.23 – 6.25) [62]. The derivative masses were obtained by comparison to the synthesized derivatives in acetone (refer to section 6.2.6).

### 6.6.5. Reaction Calibration Curves

Calibration curves for the derivatives were obtained after the *in situ* reaction with the standards of the target analytes. The underivatized alkylphenols were prepared in acetone in concentrations ranging from 5 to 80 ng/µl. 1 µl of the standard mixture was placed on the trap and allowed to evaporate. 5 µl TFAA was added to the trap and allowed to react for 10 minutes. The trap was then thermally desorbed. The quantity of derivative formed was determined by comparison with the synthesized derivatives in acetone (refer to section 6.2.6).

## 6.7. Results and Discussion

### 6.7.1. Extraction efficiency

The extraction efficiencies, obtained on different PDMS MCTs (made from 2 different PDMS batches), are summarized in table 6.7. The *tert*-octylphenol (TOP) displays good recoveries (~70-79%) on both trap batches with similar extraction efficiencies. On the first PDMS batch nonylphenol (NP) was 80% extracted. However, the second PDMS batch only extracted half that amount. In both cases the variation was large. Bisphenol-A (BPA), was poorly extracted (between

10-26%) on both PDMS batches. The poor extraction confirmed previous work performed by Nakamura *et al.* [54] using SBSE. The results of a two-tailed t-test (P=0.05) indicated that the means of the results of the 2 batches for each analyte differ significantly. The significance test can be found in appendix 4.

Extraction of analytes into PDMS can loosely be predicted by the octanol-water partition coefficient of the analyte. Typically, high extraction efficiencies are obtained for compounds with large octanol-water partition coefficients [257, 258]. BPA, despite having a relatively large octanol-water partition coefficient, does not partition well into PDMS. Extraction only improves once hydroxyl groups have been derivatized. Although designed to operate under dynamic pre-breakthrough sampling conditions (100% extraction expected) i.e. a 5 ml water sample is less than the calculated breakthrough volumes of any of the analytes, shown in table 6.5, extraction efficiencies are even less than those expected for dynamic equilibrium sampling conditions shown in table 6.3. Further work is required to investigate the reason for the low extraction efficiency observed.

In addition, table 6.7 indicates a poor reproducibility between different batches of PDMS tubing, which will require further investigation. This can be due to differences in the PDMS polymer material or to particulates in the trap. It is unlikely that particulates larger than 0.45 µm are present in the filtered MilliQ water. Other particulates may arise from dust in the laboratory.

As noted in section 6.7.2 below, the reaction efficiency data indicates that constant derivatization efficiency can be expected. We therefore assume that it too does not contribute to the observed variation. A reconstructed ion chromatogram of the raw alkylphenols' most abundant ions m/z 135 and 213 from the extraction analyses does not indicate the presence of unreacted TOP or NP, see appendix 3. As for BPA, the chromatographic run was stopped before the unreacted analyte could be detected. However, as discussed below, we would expect to see BPA since it does not convert efficiently.

**Table 6.7 Extraction efficiencies obtained for TOP, NP and BPA on 2 different PDMS MCT batches.**

| | | *tert-octylphenol TFA* | *4-n-nonylphenol TFA* | *Bisphenol-A TFA* |
|---|---|---|---|---|
| PDMS 1 | % extraction | 70 | 84 | 10 |
| | % RSD | 4 | 26 | 15 |
| | n | 7 | 8 | 8 |
| PDMS 2 | % extraction | 79 | 43 | 26 |
| | % RSD | 3 | 22 | 8 |
| | n | 5 | 5 | 5 |

### *6.7.2. Reaction efficiency*

Acetic acid anhydride is often used to convert alcoholic and phenolic functional groups into their corresponding acetates, in the presence of a base [54, 180]. The reaction is fairly quick and can take place in an aqueous medium. However, the final extraction medium is very acidic (pH 2) and causes degradation of the PDMS absorbent as observed by an increase in the siloxane degradation peaks in the chromatogram [180].

Trifluoroacetic acid anhydride (TFAA) converts the alcoholic and phenolic functional groups into their corresponding trifluoroacetate esters, with the added advantage of moving the derivatives out of the lower mass ranges and opening up detection possibilities to include electron capture and negative chemical ionization mass spectrometry. TFAA does not require a catalyst and derivatization is rapid. However, it is not suitable for use in an aqueous medium [62]. In the PDMS medium (when dry), TFAA will also form the trifluoroacetic acid by-product, however, as TFA is so volatile and unretained by the PDMS, the bulk is easily removed from the trap before thermal desorption begins.

Results obtained for the optimum reaction volume for TFAA are plotted in figure 6.31. A maximum peak area was observed when using 5 µl TFAA. It is not clear at this stage why the efficiency drops with larger volumes of reagent.

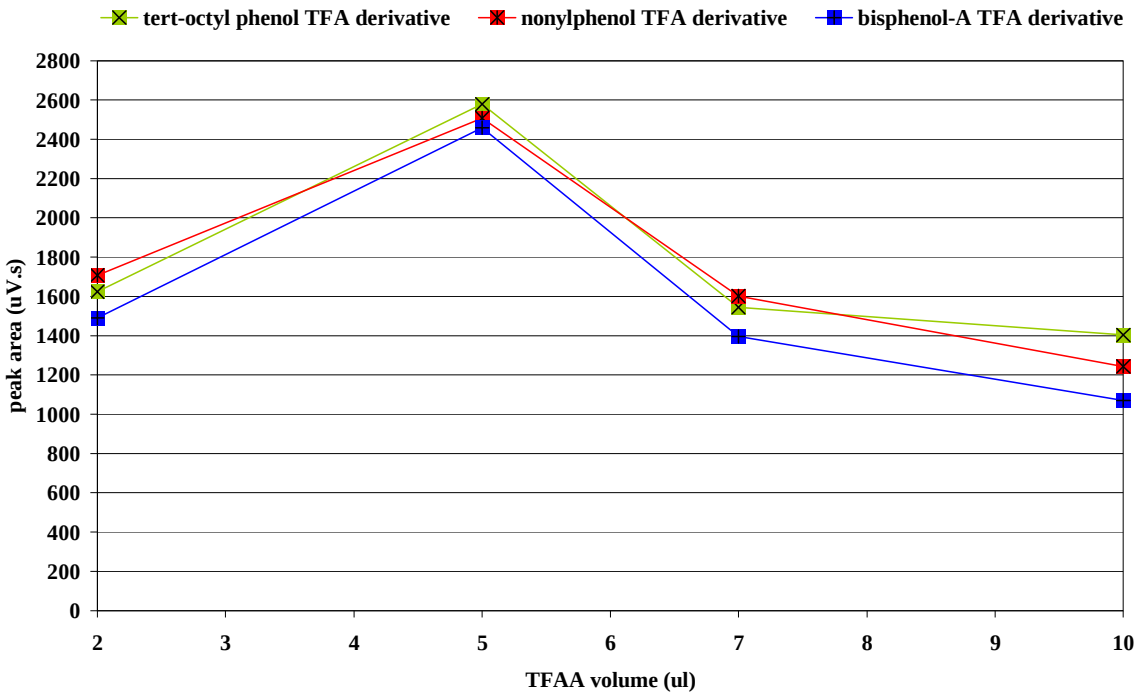


**Figure 6.31 Optimum TFAA reagent volume, determined by placing 1µl 42 ng/µl TOP, 44 ng/µl NP and 54 ng/µl BPA in acetone on the PDMS trap; the corresponding reagent volumes are added after the solvent has evaporated. The trap is then sealed with glass caps for 10 minutes before thermal desorption and analysis. The optimum TFAA volume of 5 µl was visually determined from the x-y scatter plot as the point where maximum derivative peak area is observed.**

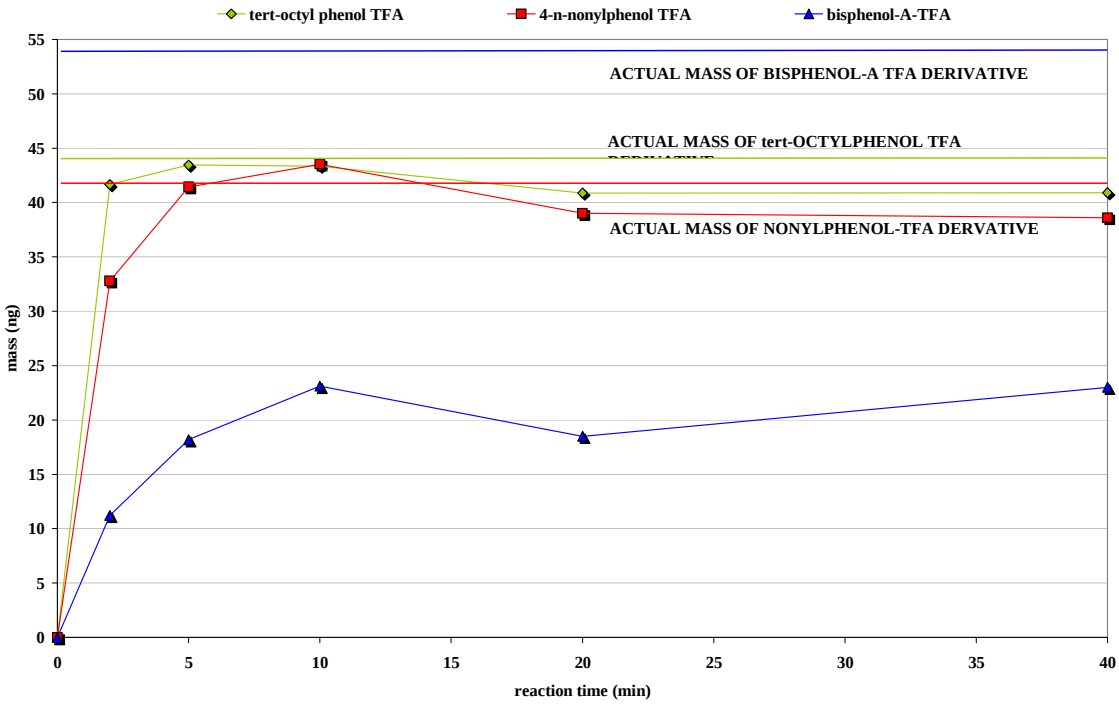


**Figure 6.32 Reaction efficiencies, determined by placing 1µl 42 ng/µl TOP, 44 ng/µl NP and 54 ng/µl BPA in acetone on the PDMS trap. 5 µl TFAA is added after the solvent has evaporated. The trap is then sealed with glass caps for the duration of the reaction. The measurement values are depicted as an x-y scatter plot with data points connected by lines. The optimum reaction time was visually determined to be 5 min, where the peak areas of the TFA-derivatives appear to reach a plateau.**

Reaction efficiencies are shown in figure 6.32. All three derivatives appear to reach a plateau after 5 minutes reaction time. This normally indicates that the reaction is complete [62]. However, a comparison of the plateau amount with the actual amount of derivative expected to form indicates that only TOP and NP have reacted completely (100%). BPA shows less than 50% reaction efficiency. Despite this the BPA-TFA derivative amount remains stable after 10 minutes and as such can still be deemed a viable reaction for the purposes of this study. The experiment was repeated and similar results were obtained as shown in appendix 3, figure A3.6. The reaction appeared complete after 5 minutes. The quantity of derivative formed was determined by comparison with the synthesized derivatives in acetone (refer to section 6.2.6).

## 6.7.3.Reaction calibration curves

Figure 6.33 shows a typical calibration curve obtained after *in situ* derivatization, using a GC-FID and one PDMS trap. Calibration using the MSD involved the confirmation with 3 ions and quantitation of the base peak ion. Table 6.8 summarises the detection limits possible with the instrumental setup used. An unexpected problem of carry-over from the thermal desorber presently limits the quantitation levels for these analytes, particularly BPA, which already suffers from poor recovery and reaction conversion. Further work in reducing the desorber contamination would be required to lower the detection limits.

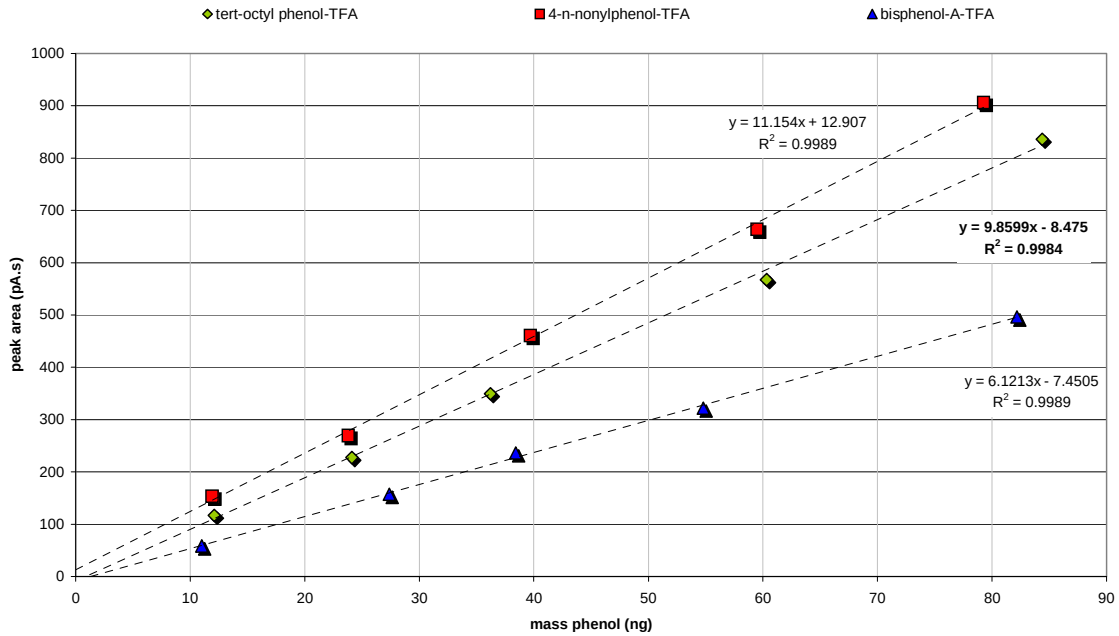


**Figure 6.33 GC-FID calibration curves obtained by the *in situ* reaction of alkylphenols on the PDMS trap.**

### *6.7.4. Minimum Detection Levels of accumulated mass*

Table 6.8 lists the Minimum Detection Levels (MDL) possible for the analytes concerned once collected on the trap. The MDLs were calculated using 1) Regression line analysis of the calibration curves [277] and 2) The instrumental signal-to-noise (s/n) ratio. The s/n detection limits are generally lower as they do not take the variability of a series of measurements into account.

As expected, the LOD (s/n =5) improves when moving from the FID to reconstructed single ion data from full scan EI-MS to selected ion monitoring EI-MS. The LOQ, using regression line analysis, for FID and full scan MS is similar as this analysis gives a better indication of the spread of measurements resulting from derivative formation and thermal desorption. The SIM LOQ is lower than the RIC LOQ, not only because of the improved s/n ratio expected from SIM but also because the thermal desorption unit was cleaned prior to measurements using SIM. Due to the number of problems experienced during this study, the final set of measurements made were those using SIM only to obtain an indication of what the best detection levels could be using a clean system. Once the underlying problems of this method are resolved, further work would be to repeat these measurements using full scan MS and SIM under consistent conditions.

The levels at which the alkylphenols and bisphenol-A can be measured using this technique are similar to the levels mentioned in the literature (see the summary presented in table 3.2.). For example, derivatization and concentration of TOP, NP and BPA in 10 ml of river water sample using acetic acid anhydride and SBSE yielded a LOD of 0.5, 5 and 2 ppt respectively by GC-SIM-MS [177]. The LOQ for TOP, NP and BPA from a 10 ml river water sample was 2, 20 and 10 ppt respectively [177]. Working with a 10 ml spiked water sample our technique can reach a LOD of 3.2, 7.1 and 20 ppt for TOP, NP and BPA respectively. However, as we are limited by background contamination our LOQ is 40, 21 and 110 ppt respectively using GC-SIM-MS. These values are based on the assumption of 100% reaction and extraction efficiencies. With the removal of background contamination detection limits can be even lower. Furthermore this technique has the added selectivity advantage of using GC-NCI-MS or GC-ECD for the detection of the electron-rich trifluoroacetate derivative as opposed to the non-halogenated acetate derivatives. The sensitivity of response of GC-NCI-MS or GC-ECD with respect to the trifluoroacetate derivatives has not been determined in this project, hence it cannot yet be established whether the increased selectivity will have a positive influence on the LOD and LOQ for these compounds.

**Table 6.8 Minimum Detection Levels. (FID = flame ionization detection, EI-RIC=electron impact reconstructed single ion, EI-SIM=electron impact selected ion monitoring, LOD=limit of detection, LOQ= limit of quantitation, LOC= level of confidence from regression line analysis, LOQ from reagent blanks (5 µl TFAA on PDMS MCT) obtained by taking the average plus three times the standard deviation of the series of measurements). The LOD (s/n =5) was determined by extrapolation from a larger signal and not from actual measurements.**

***mass (ng)***

| | 4-*tert*-octylphenol | 4-*n*-nonylphenol | bisphenol-A | |
|---|---|---|---|---|
| FID | 3.5 | 5.2 | 4.7 | LOD (s/n = 5) |
| FID | 4.1 | 3.1 | 3.1 | LOD (95% LOC) |
| FID | 14 | 10 | 10 | LOQ (95% LOC) |
| EI-RIC | 0.17 | 0.10 | 0.42 | LOD (s/n = 5) |
| EI-RIC | 0.22 | 0.16 | 0.54 | LOD (95% LOC) |
| EI-RIC | 1.6 | 5.2 | 6.7 | *LOQ (blanks n = 4)* |
| EI-RIC | 9.0 | 18 | 10 | LOQ (95% LOC) |
| EI-SIM | 0.032 | 0.071 | 0.20 | LOD (s/n = 5) |
| EI-SIM | 0.40 | 0.21 | 1.1 | *LOQ (blanks n = 4)* |

## *6.8. Limitations of this method*

### *6.8.1. PDMS degradation*

Initial water sampling experiments indicated that the PDMS MCT was severely degraded after *in situ* derivatization with the TFAA. It was found that without complete removal of water from the PDMS trap, the PDMS degradation would be significant. Figure 6.34 shows an overlaid chromatogram of two analysed PDMS MCTs that underwent *in situ* derivatization under “wet” and “dry” PDMS conditions.

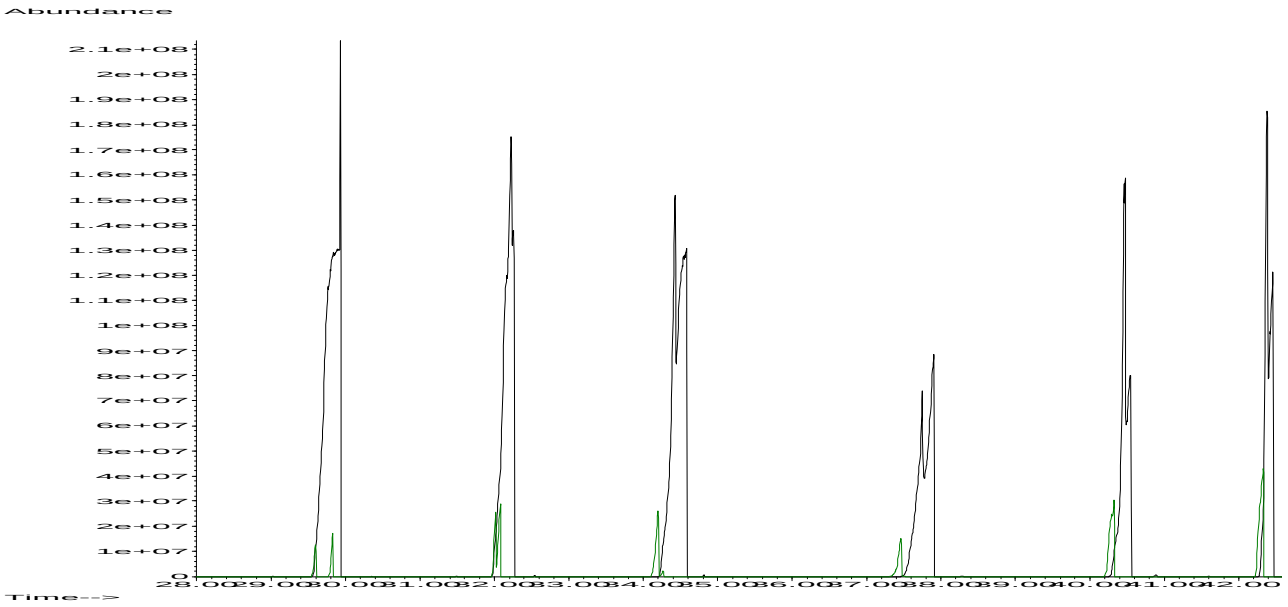


**Figure 6.34 Overlaid chromatogram of 2 PDMS MCTs. The green chromatogram is obtained after the *in situ* derivatization reaction on a "dried" trap. The black chromatogram is obtained after the *in situ* derivatization reaction on a "wet" trap.**

Under "dry" PDMS conditions, the TFA acid by-product that forms during the *in situ* derivatization reaction (figure 6.22) remains un-ionized in the gas phase; the bulk is removed from the PDMS MCT before thermal desorption occurs.

It is suspected that when the trap is "wet", the TFA acid is ionized, in the aqueous phase, to form the extremely acidic hydronium ion ($H_3O^+$) shown in figure 6.35. This hydronium ion triggers the chemical degradation of the PDMS polymer. It is suggested that this degradation, along with the usual thermal degradation of the PDMS, leads to the increased siloxane peaks observed in figure 6.34.


**Figure 6.35 Reaction equation for the TFA acid by-product in the presence of water.**

Purging the trap with nitrogen gas after centrifuging (the method suggested by Ortner [63]) did not remove all the water. However, in Ortner's [63] case removal of all the water was not critical. Physically tapping water out of the trap by dropping it several times down a 1.5 m long tube, helped to remove the water droplets that were trapped through capillary action inside the PDMS channels.

Followed by a 1 min high flow (approximately 1L/min) purge with hydrogen gas, this process removed most of the water from the trap. See appendix 5 for the trap drying investigation results.

The best results were obtained when the trap was capped with dried silica gel for approximately 2 hours or left overnight. This last step removed any residual vapour caught in the PDMS matrix. Removal of the residual water vapour could not be determined gravimetrically, see appendix 5. The only indication that all the water vapour had been removed was through the *in situ* derivatization in the PDMS. When the size of the PDMS degradation peaks resulting from a PDMS MCT having undergone *in situ* derivatization did not differ much from the PDMS degradation peaks resulting from a PDMS MCT blank desorption run, we assumed that all the water had been removed. As discussed in chapter 2 (Section 2.6), the PDMS matrix is not 100% pure PDMS, but contains up to 40% fumed silica ($SiO_2$) as filler. It is possible that the $SiO_2$ holds the residual water vapour in the PDMS matrix, since it is known that pure PDMS is a hydrophobic polymer.

It should also be noted that analytes, with boiling points in the C16 to C20 range, are not volatile enough to be removed from the trap during the high-speed gas-purging step at room temperature. This step should be of concern only when working with analytes that have low retention volumes or high volatilities.

### *6.8.2. Desorber contamination*

As can be seen in figure 6.36, from the system blank chromatogram obtained from desorption of an empty glass tube that desorber contamination has occurred as a result of sample carry-over. This persistent carry-over limits the minimum possible levels of detection for the analytes being determined, see table 6.8.

After the thermal desorption phase in the Gerstel® desorption unit (see figure 4.3), the tube desorption chamber is cooled down from 260ºC to the initial temperature of 40ºC, before the CIS is ramped to desorb the cryogenically trapped analytes from the baffled glass inlet.

It is suspected that sample carry-over occurs inside the TDS tube desorption chamber (see figure 4.3) during this cooling phase. Despite a permanent carrier gas purge flow of 3 ml/min around the desorption tube, the underivatized analytes and particularly the TFA acid by-product can condense onto the metal surfaces inside the chamber where they are desorbed during future desorption cycles. An improvement in background levels was observed when this chamber was cleaned out with

methanol. Another possible solution to this problem is to increase the purge flow around the tube manually.

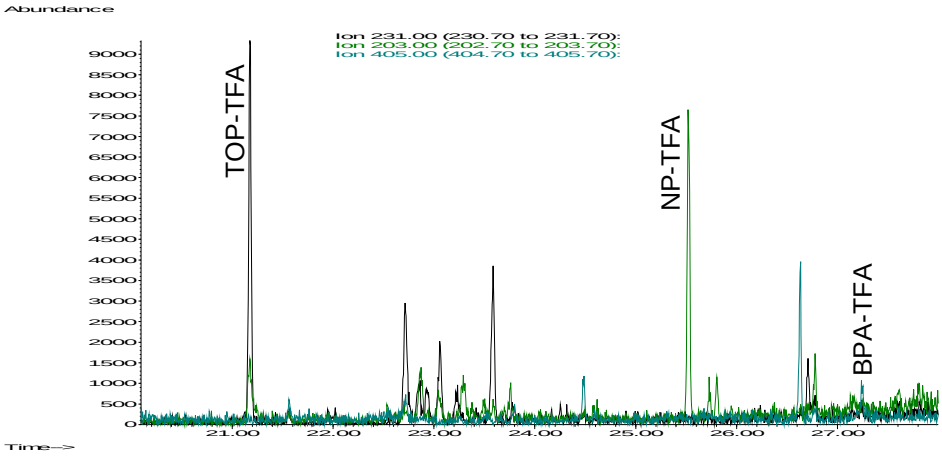


**Figure 6.36 System blank reconstructed ion chromatogram obtained from desorption of an empty glass tube. *Tert*-octylphenol trifluoroacetate derivative (TOP-TFA) m/z 231, $t_R$ = 21.2 min; 4-*n*-nonylphenol trifluoroacetate derivative (NP-TFA) m/z 203, $t_R$ = 25.6 min; bisphenol-A trifluoroacetate derivative (BPA-TFA) m/z 405, $t_R$ = 27.2 min.**

## *6.9. Spiked water samples*

Figure 6.37 depicts the TFAA reagent blank (A) and a 5 ml water sample spiked with 1µl of a 25 ng/µl of the alkylphenols and bisphenol-A in methanol (B). Figure 6.37 (C) shows the extracted ion chromatogram for the base peak ions of each derivative, namely: m/z 231 (TOP-TFA), m/z 203 (NP-TFA) and m/z 405 (BPA-TFA). The procedures for extraction and reaction are as described above in sections 6.6.3 and 6.6.4.

## *6.10. Real water samples*

Water samples were brought to the lab for preliminary testing. Once the method has been improved upon, further work would include on-site extraction of water samples using the PDMS MCT.

All water samples analysed used the same procedure (described in sections 6.6.3 and 6.6.4 above) for testing the extraction and reaction efficiencies. However, a sample size of 20 ml was used instead of 5 ml. This still falls within the expected breakthrough volumes of the analytes under test (see table 6.5.).

The first 5 L sample was taken from the Apies River, downstream from a sewage treatment plant. The second 5 L sample was taken from the river at the LC de Villiers Sports Centre at the University of Pretoria. In both cases, the bottle openings were covered with aluminium foil before sealing with screw-on caps. Upon reaching the lab, methanol (100 ml) was added to the bottle to prevent adsorption of phenolic compounds on any active glass surfaces. Methanol, often 5 % of the sample volume, is added to water samples to prevent adsorption of analytes on active glass surfaces [47, 63, 278]. However, Lee *et.al*, found that adding methanol to the sample reduced the extraction yield of 4-nonylphenol using SBSE. As a point of departure, we opted for adding 2% methanol as modifier to the water sample, as a precautionary measure against larger losses due to adsorption. 20 ml aliquots were taken, using a glass pipette, for PDMS concentration. Both samples were analysed within 48 hours. The quantitative results are summarised in table 6.9.

Figures 6.38 and 6.40 show the results obtained for 2 aliquots of the Apies river water sample extracted and derivatized on 2 different PDMS MCTs. Figure 6.39 shows the reagent blank. All 3 figures show the total ion chromatogram, followed by the extracted PDMS degradation peaks (note the repeatable retention times) and the extracted derivative ions. It is obvious that the reagent blank is not “blank” since the system is contaminated. What is also of concern is that 2 aliquots analysed on 2 different traps gave 2 different sets of results. Interestingly, only the amounts determined for bisphenol-A fall below the limits of quantification (LOQ) (see table 6.9.). Both TOP and NP are detected in the sample above levels detected in the blank. This can be observed visually by inspection of the respective peaks on the blank and sample chromatograms and quantitatively by comparison with external standard calibration curves.

Figures 6.41 and 6.42 present the results obtained for the reagent blank and a 20 ml aliquot of the second sample taken from the Sports Centre river site. These results were obtained by operating the mass spectrometer in selected ion mode (SIM) using the base peaks and more abundant ions for each derivative. Masses 231, 203, 245, 316, 405, 420 were selected for SIM. Once again, only the quantities obtained for bisphenol-A fall below the LOQ.

Note the LOQ(RIC) values were determined before the TDS was cleaned. The LOQ(SIM) values are still limited by carry-over but were determined after the TDS was cleaned, hence the lower value. The process of determining LOQs must be determined under identical conditions once the continuous sample carry-over problem is resolved. It is not practical to keep cleaning the TDS chamber after each measurement.

It was also observed that with continued use and degradation of the PDMS traps, more peaks would appear in the chromatograms that contained ions related to PDMS and to the derivatives, probably indicating that side products were starting to form with the PDMS degradation products and the TFAA reagent. This is particularly noticeable in SIM where peaks with the selected ion masses were eluting at the PDMS peak retention times. Bisphenol-A, for example, has a peak eluting before and after its own peak at 27.2 min. It can be assumed that these are isomers of BPA. However, the presence of siloxane masses in the mass spectrum indicates that it is not the case. In addition, the ratios of the ions m/z 405 to m/z 420 (the base peak and molecular ions) are different from the BPA-TFA derivative. Peak one (ratio 10:1) BPA-TFA peak (ratio 7:1) and peak 2 (ratio 13:1).

**Table 6.9 Quantitative results obtained for 20 ml real samples by external standard calibration, after subtraction of the blank value. Concentration values based on 100% reaction and extraction efficiencies. Corrected concentration values obtained through inclusion of extraction and reaction efficiency factors (PDMS batch 2). TOP (100% reaction, 79 % extraction); NP (100% reaction, 43% extraction) and BPA (37% reaction, 26% extraction). Analyte concentrations below LOQ are not listed.**

| | | TOP | NP | BPA | |
|---|---|---|---|---|---|
| | **m/z** | **231** | **203** | **405** | |
| | **LOQ (RIC)** | **0.079** | **0.26** | **0.33** | **ppb** |
| RIC | APIES river - sample 1 | 1.3 | 0.93 | - | conc. |
| | | *1.7* | *2.2* | - | *corrected conc.* |
| | APIES river - sample 2 | 0.63 | 1.7 | - | conc. |
| | | *0.80* | *3.9* | - | *corrected conc.* |
| | **LOQ (SIM)** | **0.020** | **0.011** | **0.054** | **ppb** |
| SIM | LC river - sample 1 | 0.091 | 0.19 | - | conc. |
| | | *0.12* | *0.45* | - | *corrected conc.* |
| | LC river - sample 2 | 0.26 | 0.025 | - | conc. |
| | | *0.33* | *0.058* | - | *corrected conc.* |

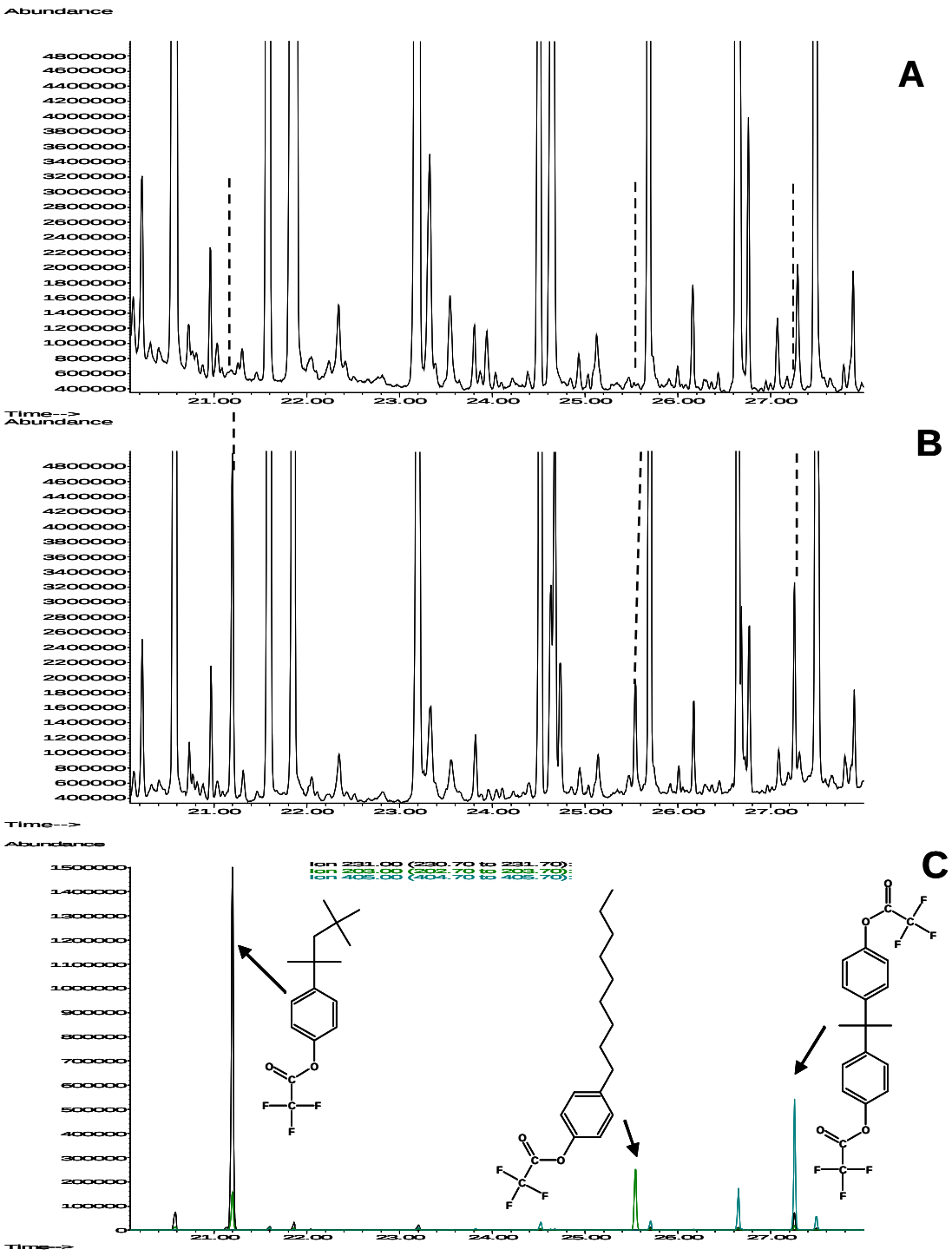


**Figure 6.37 (A) Total ion chromatogram of the reagent blank.**

**Figure 6.37 (B) Total ion chromatogram of a 5 ml MilliQ water sample spiked with 25 ng alkylphenol standard in methanol, sampled through the PDMS MCT (50 µl/min), dried and allowed to react with 5 µl trifluoroacetic acid anhydride for 10 min, followed by thermal desorption. Figure 6.37 (C) The extracted ion chromatogram of the base peak ions used for quantitation. *Tert*-octylphenol trifluoroacetate derivative (TOP-TFA) m/z 231, $t_R$ = 21.2 min; 4-*n*-nonylphenol trifluoroacetate derivative (NP-TFA) m/z 203, $t_R$ = 25.6 min; bisphenol-A trifluoroacetate derivative (BPA-TFA) m/z 405, $t_R$ = 27.2 min.**

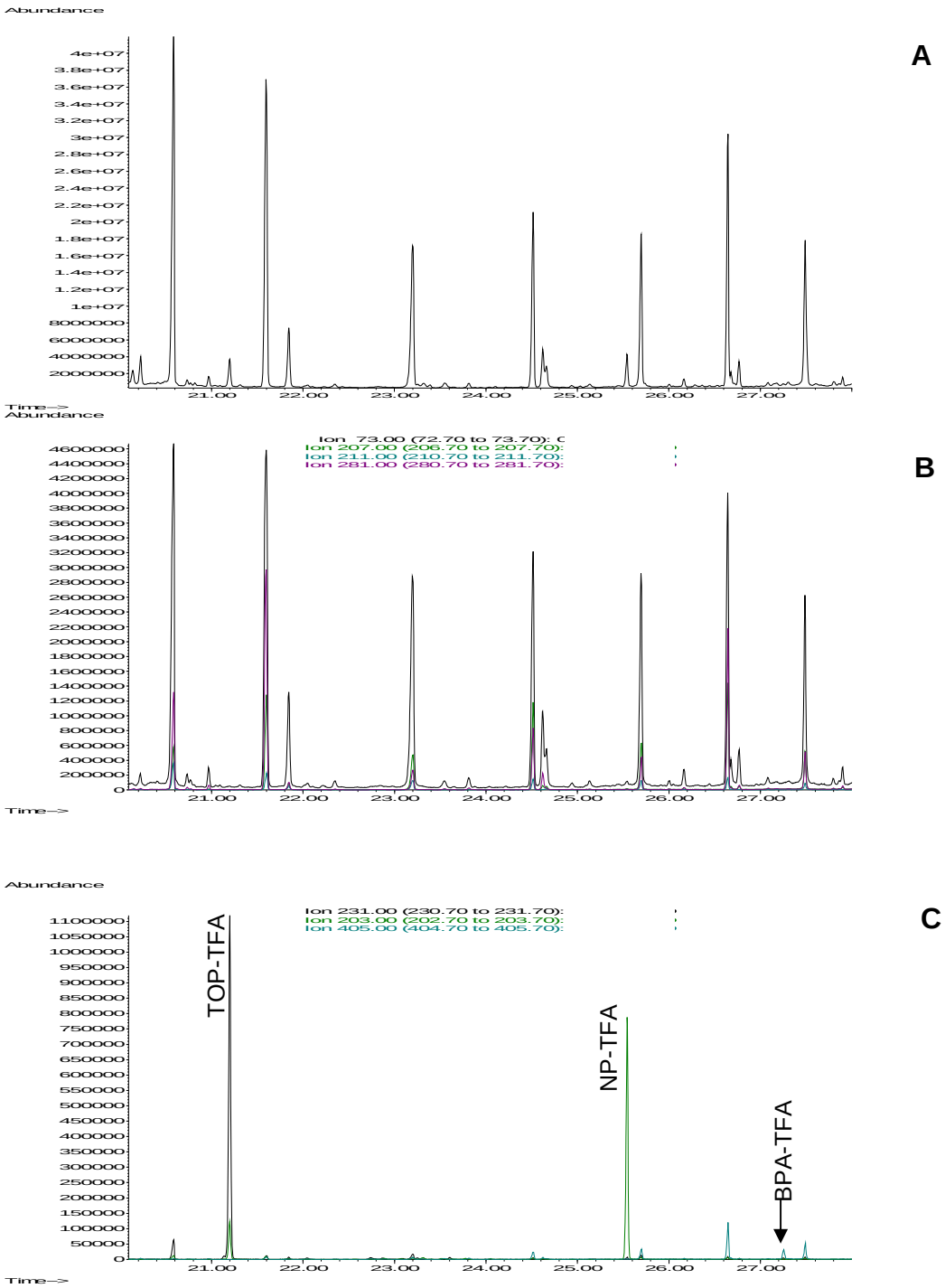


**Figure 6.38 (A) Total ion chromatogram of the 20 ml Apies River water sample on PDMS MCT M1.Sample extracted at a flow rate of 50 µl/min, dried and allowed to react with 5 µl trifluoroacetic acid anhydride for 10 min, followed by thermal desorption.**

**Figure 6.38 (B) Extracted ion chromatogram of PDMS degradation peaks m/z 73, 207, 211 and 281. Figure 6.38 (C) Extracted ion chromatogram of the base peak ions used for quantitation. *Tert*-octylphenol trifluoroacetate derivative (TOP-TFA) m/z 231, $t_R$ = 21.2 min; 4-*n*-nonylphenol trifluoroacetate derivative (NP-TFA) m/z 203, $t_R$ = 25.6 min; bisphenol-A trifluoroacetate derivative (BPA-TFA) m/z 405, $t_R$ = 27.2 min.**

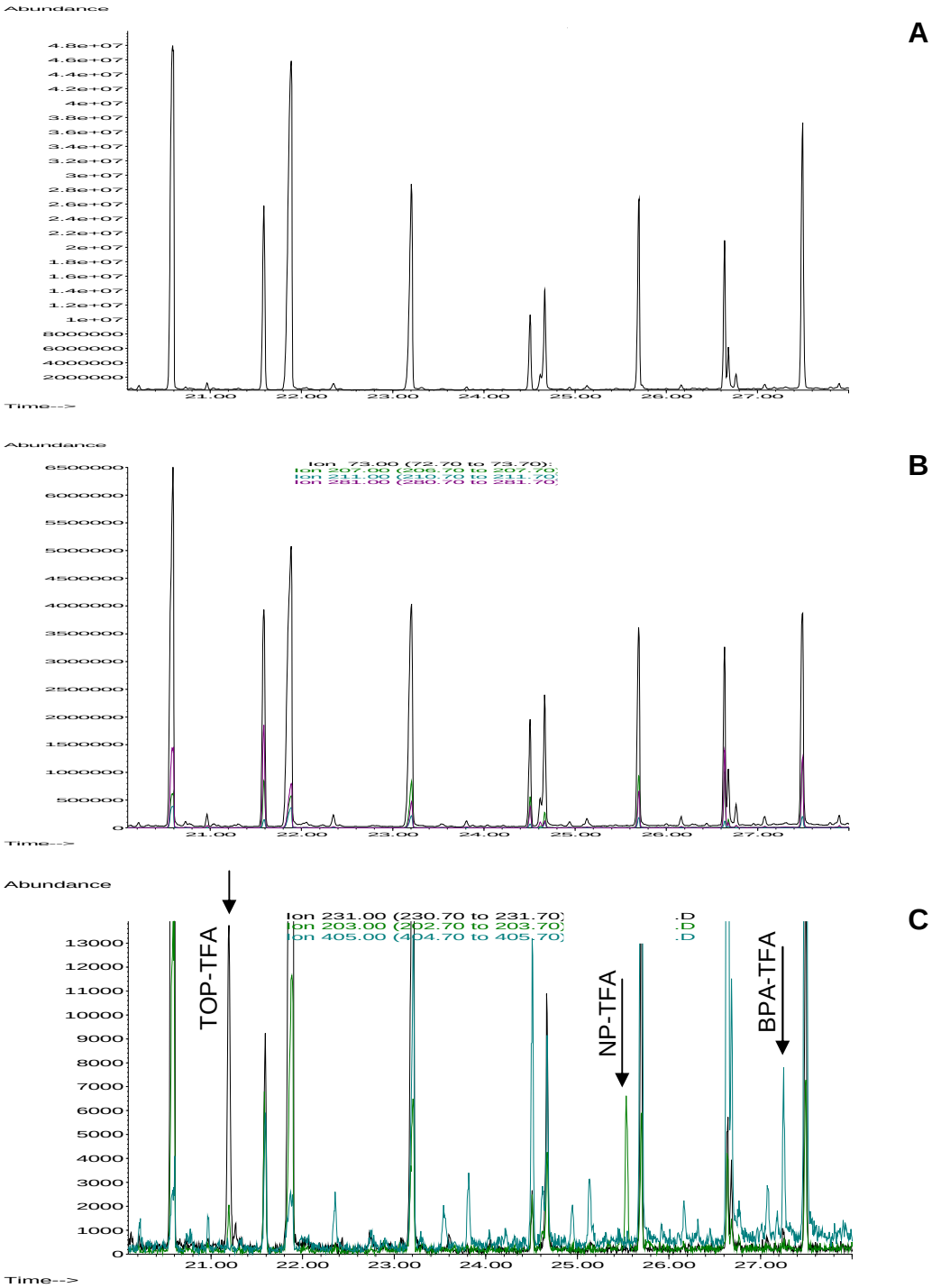


**Figure 6.39 (A) Total ion chromatogram of the TFAA reagent blank on PDMS MCT M1. 5 µl trifluoroacetic acid anhydride placed on trap for 10 min, followed by thermal desorption. Figure 6.39 (B) Extracted ion chromatogram of PDMS degradation peaks m/z 73, 207, 211 and 281.**

**Figure 6.39 (C) Extracted ion chromatogram of the base peak ions used for quantitation. *Tert*-octylphenol trifluoroacetate derivative (TOP-TFA) m/z 231, $t_R$ = 21.2 min; 4-*n*-nonylphenol trifluoroacetate derivative (NP-TFA) m/z 203, $t_R$ = 25.6 min; bisphenol-A trifluoroacetate derivative (BPA-TFA) m/z 405, $t_R$ = 27.2 min.**

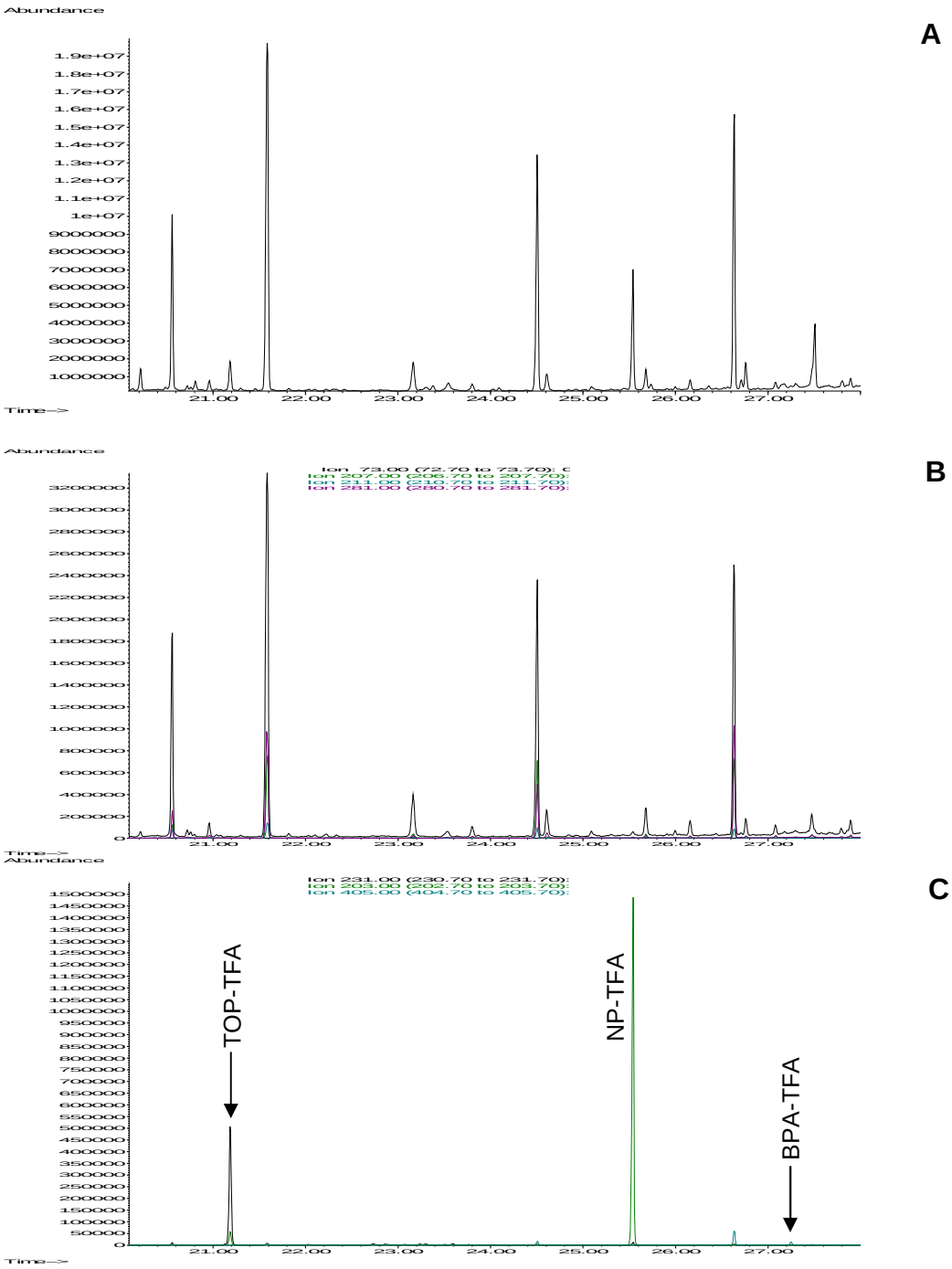


**Figure 6.40 (A) Total ion chromatogram of the 20 ml Apies River water sample on PDMS MCT M2.**

**Sample extracted at a flow rate of 50 µl/min, dried and allowed to react with 5 µl trifluoroacetic acid anhydride for 10 min, followed by thermal desorption.**

**Figure 6.40 (B) Extracted ion chromatogram of PDMS degradation peaks m/z 73, 207, 211 and 281.**

**Figure 6.40 (C) Extracted ion chromatogram of the base peak ions used for quantitation. *Tert*-octylphenol trifluoroacetate derivative (TOP-TFA) m/z 231, $t_R$ = 21.2 min; 4-*n*-nonylphenol trifluoroacetate derivative (NP-TFA) m/z 203, $t_R$ = 25.6 min; bisphenol-A trifluoroacetate derivative (BPA-TFA) m/z 405, $t_R$ = 27.2 min.**

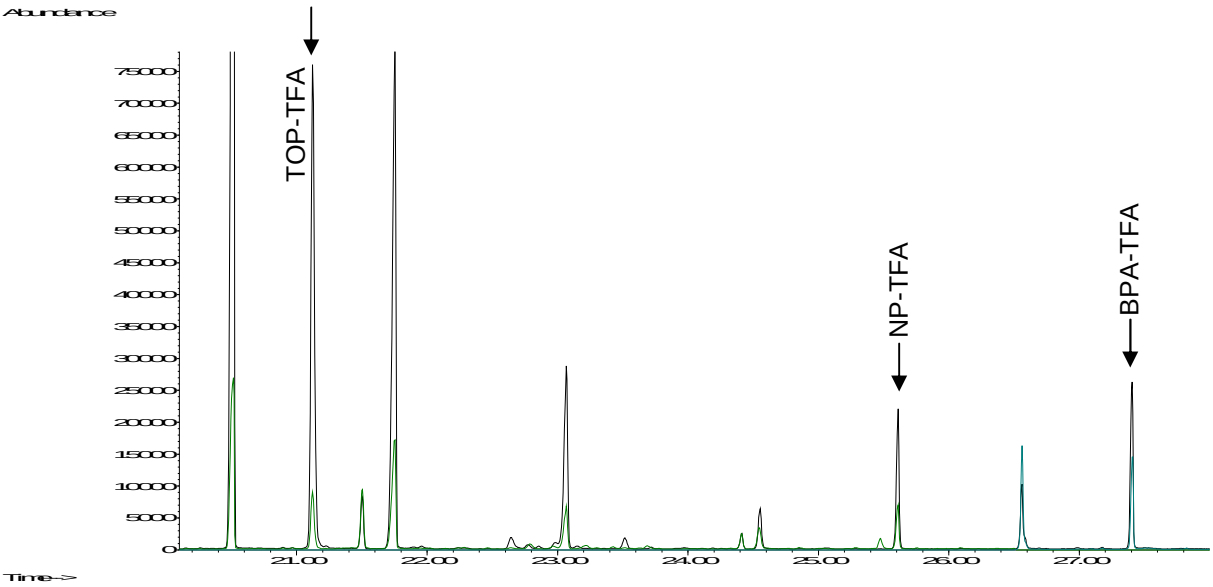


**Figure 6.41 Selected Ion Mode (SIM) chromatogram of the TFAA reagent blank on PDMS MCT M3. Selected ions were m/z 231, 203, 245, 316, 405, 420. 5 µl trifluoroacetic acid anhydride placed on trap for 10 min, followed by thermal desorption. *Tert*-octylphenol trifluoroacetate derivative (TOP-TFA) m/z 231, $t_R$ = 21.2 min; 4-*n*-nonylphenol trifluoroacetate derivative (NP-TFA) m/z 203, $t_R$ = 25.6 min; bisphenol-A trifluoroacetate derivative (BPA-TFA) m/z 405, $t_R$ = 27.2 min.**

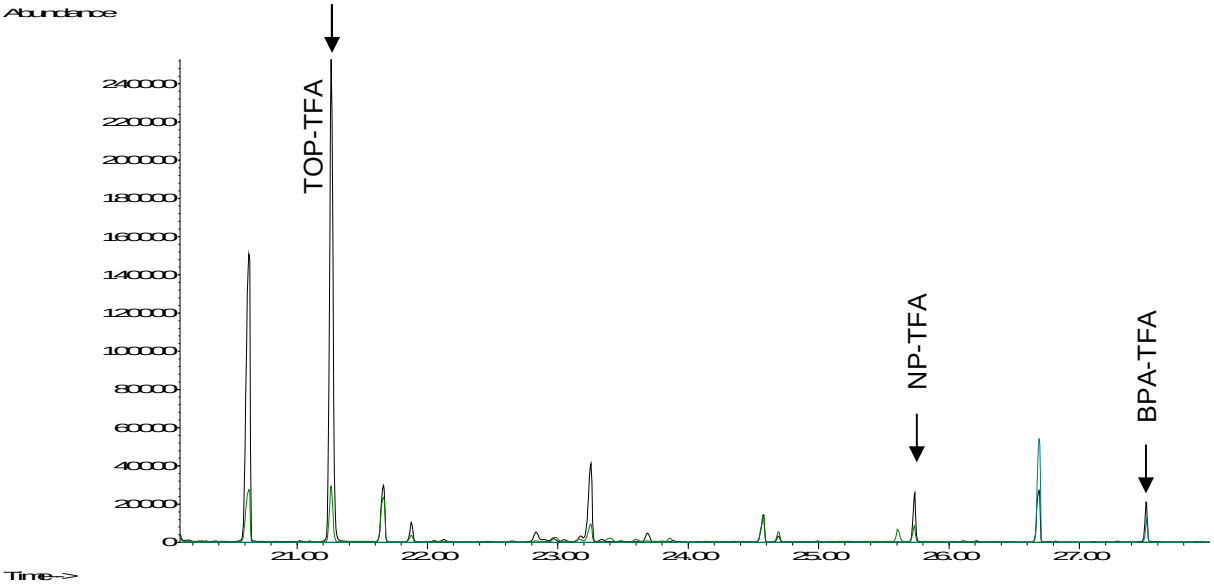


**Figure 6.42 Selected Ion Mode (SIM) chromatogram of the 20 ml UP Sports Centre river water sample on PDMS MCT M3. Sample extracted at a flow rate of 50 µl/min, dried and allowed to react with 5 µl trifluoroacetic acid anhydride for 10 min, followed by thermal desorption. Selected ions were m/z 231, 203, 245, 316, 405, 420. *Tert*-octylphenol trifluoroacetate derivative (TOP-TFA) m/z 231, $t_R$ = 21.2 min; 4-*n*-nonylphenol trifluoroacetate derivative (NP-TFA) m/z 203, $t_R$ = 25.6 min; bisphenol-A trifluoroacetate derivative (BPA-TFA) m/z 405, $t_R$ = 27.2 min.**

## 6.11. Conclusion

The multichannel PDMS trap can be used to extract the moderately polar *tert*-octyl phenol and nonylphenol directly from water and can serve as a "one-pot" concentration, transport, derivatization and desorption vessel.

An extraction efficiency of over 70% is obtained for *tert*-octylphenol. However, extraction of nonylphenol and bisphenol-A is not as reproducible between different PDMS batches. A deviation from the expected partitioning of these lipophillic compounds, based on calculations using their octanol-water partitioning coefficients, is evident. Only ~40% nonylphenol and ~20% bisphenol-A partitions into the PDMS, while 99% partitioning is expected.

The *in situ* derivatization reaction, using only 5 µl of trifluoroacetic acid anhydride, is convenient as it occurs at room temperature in the PDMS trap and is 100% complete within 10 minutes for *tert*-octylphenol and nonylphenol. Bisphenol-A demonstrates a modest reaction efficiency of approximately 37%, however, this appears to be constant over time.

Analyte carry-over from the thermal desorber presently prevents the achievement of further reduction in detection levels expected when moving from GC-EI-MS to GC-NCI-MS. Despite this, minimum detectable levels are similar to those achieved in the literature. The limit of quantitation (determined by the reagent blank) for this technique using GC-SIM-MS are 20, 11 and 54 ppt for *tert*-octylphenol, nonylphenol and bisphenol-A respectively.

The ability of the PDMS MCT to concentrate alkylphenols directly from water followed by *in situ* derivatization using TFAA, was demonstrated on real samples brought into the laboratory. Both *tert*-octylphenol and nonylphenol were detected in all samples at the low ppb level, while bisphenol-A fell below the level of quantitation. Once background levels are reduced, on-site sampling with the PDMS MCT would still need to be tested.